**Report No: GESAC-01-04**

# BIOMECHANICAL RESPONSE REQUIREMENTS OF THE THOR NHTSA ADVANCED FRONTAL DUMMY

**(Revision 2001.02)**

## TRAUMA ASSESSMENT DEVICE DEVELOPMENT PROGRAM

**Revised: November, 2001**

Prepared under contract DTNH22-94-C-07010 for the National Transportation Biomechanics Research Center, Office of Human-Centered Research, National Highway Traffic Safety Administration, U.S. Department of Transportation

---

GESAC

General Engineering and Systems Analysis Company, Inc
125 Orchard Drive
Boonsboro, MD 21713

# BIOMECHANICAL RESPONSE REQUIREMENTS OF THE THOR NHTSA ADVANCED FRONTAL DUMMY

# BIOMECHANICAL RESPONSE REQUIREMENTS OF THE THOR NHTSA ADVANCED FRONTAL DUMMY

## 1. INTRODUCTION

This report constitutes part of the final documentation for the NHTSA Advanced Frontal Dummy known as THOR (**T**est device for **H**uman **O**ccupant **R**estraint). It describes the biomechanical response requirements which have been defined to assess the biofidelity of the Thor dummy. The report also provides results from tests performed to evaluate the level of agreement with these requirements. A summary of the test procedures used for testing Thor with respect to the requirements are given, but the exact details of the testing procedures will be found in the Thor Certification Manual which is a part of the Thor documentation. In addition, the report proposes a number of additional requirements, which will assess the biofidelity of Thor in a number of test environments which were not covered by the first set of requirements.

The report is arranged in three sections. In each section, the report is arranged according to the principal segments of the dummy. Section I contains the requirements that were defined during the initial design, fabrication, and testing of the dummy. These requirements have been available for some time and the response of the Thor dummy has been tested against these requirements during an extensive test program. For each segment, the sources of background information are provided, followed by a brief description of the experimental procedure, and finally, the target biomechanical response is presented.

Section II presents the results from testing performed on Thor to evaluate the biofidelity of the dummy with respect to the biomechanical requirements.

Section III contains requirements that have been more recently proposed and includes data gathered from more recent biomechanical research. The Thor dummy has either been tested only in a limited way, or not at all, against these newer requirements. Elements of these requirements may be adopted in fully qualifying the Thor ATD.

In Section I, biomechanical response requirements for the following segments are described.

| | | | |
|---|---|---|---|
| 1. | Head | - | Based on cadaver drop tests by Hodgson and Thomas, and impact tests at UMTRI |
| 2. | Neck | - | Dynamic neck bending responses for frontal and lateral flexion based on tests performed at Naval Biodynamics Laboratory and kinematic data developed by TNO, and moment-angle relations developed by Mertz, Patrick, and Chou. |
| 3. | Thorax | - | Upper ribcage requirement based on force-deflection data developed by Neathery based on testing by Kroell ; lower ribcage requirement based on force-deflection data developed by MCW. |
| 5. | Abdomen | - | Lower abdomen force-penetration data based on low severity impacts carried out by Cavanaugh; upper abdomen force-penetration data based on impacts carried out by Nusholtz. |

| | | | |
|---|---|---|---|
| 6. | Femur | - | Based on knee impact tests performed and analyzed by Horsch and Patrick. |
| 7. | Face | - | Based on impact tests by Nyquist, Allsop, and Melvin and analyzed by Melvin. |
| 8. | Lower Leg | - | Dorsiflexion response from dynamic tests performed by Renault, leg axial response from dynamic tests performed by MCW, and a number of quasi-static responses in dorsiflexion, plantarflexion, inversion, and eversion, performed by UVa and Renault. |

In Section II, as indicated above, the results from testing Thor according to the requirements outlined in Section I are presented.

In Section III, the proposed., additional response requirements are described.

| | | | |
|---|---|---|---|
| 1. | Neck | - | Dynamic neck bending response in extension based on tests performed by TNO and moment-angle relations developed by Mertz and Patrick. Secondary requirements based on compression, tension, and torsion response. |
| 2. | Spine | - | No biomechanical requirements currently defined. |
| 3. | Thorax | - | Quasi-static localized response data based on testing by Cavanaugh, and belt impact response based on testing by INRETS. |
| 4. | Abdomen | - | Force-deflection response for belt and airbag interaction with abdomen based on testing by UMTRI. |
| 5. | Face | - | Additional requirements based on more localized testing by INRETS. |
| 6. | Lower Leg | - | Dynamic inversion/eversion response based on testing by Renault. |

## SECTION I. CURRENT BIOMECHANICAL REQUIREMENTS

## 2. HEAD

### References

Hodgson, V., Thomas, L. 1975. *Head impact response.* Vehicle Research Institute, Rpt VRI 7.2. SAE, Warrendale, PA.
Melvin, J., Weber, K. 1985. *Task B Final Report.* DOT HS 807 042. NHTSA.
Prasad, P., Melvin, J., Huelke, D., King, A., Nyquist, G. 1985. *Head. Review of Biomechanical Impact Response and Injury in the Automotive Environment.* pp 1-43. Ed. J.

### Description

The response of the head to frontal impact is based on two sets of tests. Response to lower velocity impacts (at 2.0 m/s) is based on the non-fracture head impact tests of Hodgson and Thomas at Wayne State University [1975]. Response to higher velocity impacts (at 5.5 m/s) is based on the non-fracture head impact tests at UMTRI [Prasad, et al; 1985]. Melvin [1985] proposed an equivalent procedure which equated the impact energy in the head drop tests, with the effective impact energy from an impactor test on the forehead of a complete dummy. The procedure developed by Melvin has been selected to establish the biofidelity of Thor under head impact. This procedure has some advantages over the normal head drop test. The problems of orienting the head during a head drop test are avoided. In addition, the biofidelity of impacts to the lateral aspect of the head is simpler to evaluate, as it requires a simple rotation of the dummy. The priority will be given to meeting the response for impact velocity of 2.0 m/s.

### Test Setup

1. The subject is set up in a sitting position, with its legs horizontal and the arms raised (may be taped lightly to a support bar).
2. Impactor mass is 23.4kg. The impact surface is rigid and flat, with a diameter of 15.2 cm.
3. The impact speeds are 2.0 m/s and 5.5 m/s.
4. The head of the dummy is placed, such that the axis of the impactor is aimed at a point on the forehead on the midsagittal plane and 30 mm above the horizontal line marking the division with the face skin. The tilt of the dummy head/neck assembly is adjusted so that the impact area on the head is parallel to the face of the impactor.

### Biomechanical Response

The corridors are described as a force vs duration time response for the two impact speeds and are shown in Figure 1.

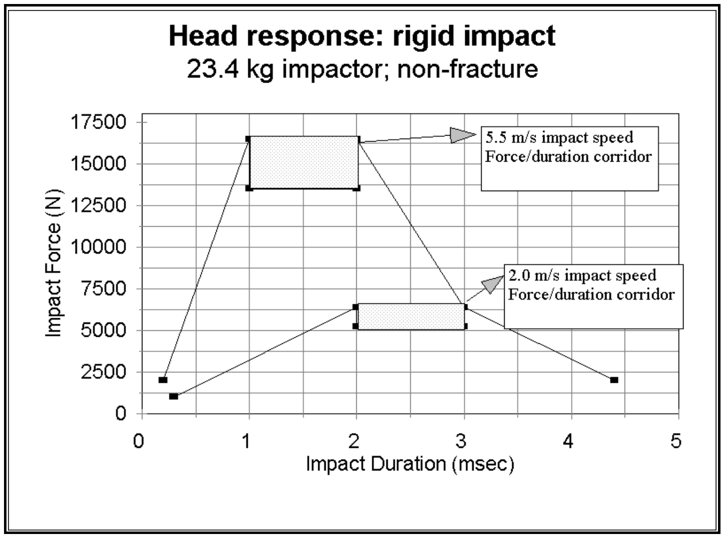


**Figure 1. Non-fracture response of head for impact with rigid surface [Melvin, 1985]**

# 3. NECK

## References

Ewing, C.L., Thomas, D.J., Beeler, G.W., Patrick, L.M., and Gillis, D.B. 1968. *Dynamic Response of the Head and Neck of the Living Human to -Gx Impact Acceleration.* Twelfth Stapp Car Crash Conference. SAE Paper # 680792.
Ewing, C.L., Thomas, D.J., Patrick, L.M., Beeler, G.W., and Smith, M.J. 1969. *Living Human Dynamic Response to -Gx Impact Acceleration, Part II - Accelerations Measured on the Head and Neck.* Thirteenth Stapp Car Crash Conference.
Ewing, C.L., and Thomas, D.J. 1973. *Torque Versus Angular Displacement Response for the Human Head to -Gx Impact Acceleration.* Seventeenth Stapp Car Crash Conference. SAE 730976.
Ewing, C.L., Thomas, D.J., Lustick, L., Becker, E., Willems, G., and Muzzy, W.H. 1975. *The Effect of the Initial Position of the Head and Neck on the Dynamic Response of the Human Head and Neck to -Gx Impact Acceleration.* Nineteenth Stapp Car Crash Conference. SAE Paper # 751157.
Ewing, C.L., Thomas, D.J., Lustick, L., Muzzy, W.H., Willems, G., and Majewski, P.L. 1976. *The Effect of Duration, Rate of Onset and Peak Sled Acceleration on the Dynamic Response of the Human Head and Neck.* Twentieth Stapp Car Crash Conference. SAE Paper # 760800.
Ewing, C.L., Thomas, D.J., Majewski, P.L., Black, R., and Lustick, L. 1977. *Measurement of Head, T1, and Pelvic Response to -Gx Impact Acceleration.* Twenty-First Stapp Car Crash Conference. SAE Paper # 770927.
Klinich, K., Beebe, M., Pritz, H., and Haffner, M. 1995. *Performance Criteria for a Biofidelic Dummy Neck.* National Highway Traffic Safety Administration, Vehicle Research and Test Center.
Mertz, H.J. and Patrick, L.M. 1971. *Strength and Response of the Human Neck.* Fifteenth Stapp Car Crash Conference. SAE Paper # 710855.
Patrick, L.M., and Chou, C.C. 1976. *Response of the Human Neck in Flexion, Extension and Lateral Flexion.* Vehicle Research Institute Report VRI 7.3.
Thunissen, J. et al. 1995. *Human Volunteer Head-Neck Response in Frontal Flexion: A New Analysis.* Thirty-ninth Stapp Car Crash Conference. SAE Paper # 952721.
Wismans, J., and Spenny, C.H. 1983. *Performance Requirements for Mechanical Necks in Lateral Flexion.* Twenty-seventh Stapp Car Crash Conference. SAE Paper # 831613.
Wismans, J., and Spenny, C.H. 1984. *Head-Neck Response in Frontal Flexion.* Twenty-eighth Stapp Car Crash Conference. SAE Paper # 841666.
Wismans, J. et al. 1987. *Comparison of Human Volunteer and Cadaver Head-Neck Response in Frontal Flexion.* Thirty-first Stapp Car Crash Conference. SAE Paper # 872194.

## 3.1 Neck Kinematic and Dynamic Requirements in Frontal Flexion

### Description

The frontal flexion requirements arose from the extensive tests conducted by Ewing, et al. [1968, 1969, 1973, 1975, 1976, 1977]. These data were later analyzed by Wismans and Spenny [1983, 1984, 1987], from which the final form of the requirements were developed. In the original NBDL tests, two sled acceleration levels, at 15 G and 8 G, were used to develop responses for sagittal flexion. The response at the more severe 15 G level will be the primary response required to be met, since this is closest to the T1 accelerations that will be encountered with decelerations generated at typical 48 kph or 56 kph impact speeds. T1 accelerations at these severities may be around 40 G.

The neck response is primarily prescribed by the time histories of the head rotation angle and the longitudinal and vertical displacements of the head C.G. The latest revisions to the corridors for the 15 G input pulse have been presented by Thunissen, et al. [1995]. These are similar to the requirements proposed by Klinich et al. [1995], which had formed the basis of an earlier requirement, and is still used for defining the lateral flexion response.

In addition to primary responses described above, the resultant acceleration of the head C.G. as defined by Thunissen is also used as kinematic requirement. For the dynamic requirement, the moment-angle response at the occipital condyle [O.C.] described originally by Mertz and Patrick [1971], is used.

**Test Setup**

The neck flexion tests were performed on the NBDL volunteers, according to the following procedure:

1. The subject is seated upright on the sled.
2. Subjects restrained by pair of shoulder belts, a lap belt, and an inverted-V pelvic strap tied to the lap belt.
3. The motion of the sled is adjusted to have a acceleration curve shown in Figure 2.
4. Target markers and accelerometers were used to record the kinematic and dynamic responses of the subject.

For testing the biofidelity of the Thor neck, the procedure is simplified by testing the head and neck assembly only, with the base of the neck being directly attached to a sled apparatus (optionally through a lower neck load cell) that can duplicate the acceleration pulse seen at the T1 location. There will be some discrepancy with the whole-body test, since the rotation at T1, seen in the volunteer testing, cannot be generated with this procedure. As indicated in Thunissen [1995], the error in neglecting T1 rotation is estimated to be small.

**Biomechanical Requirement**

The input acceleration pulse at T1 is shown in Figure 2 and the original sled pulse is shown in Figure 3 for reference. The responses for the 15 G frontal flexion test are shown in Figures 4 to 7.

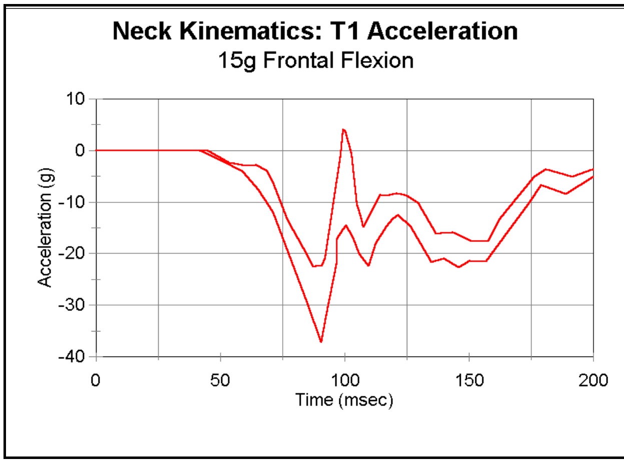


Figure 2. Input acceleration pulse for 15 G frontal flexion test of neck (equivalent to T1 acceleration of volunteers).

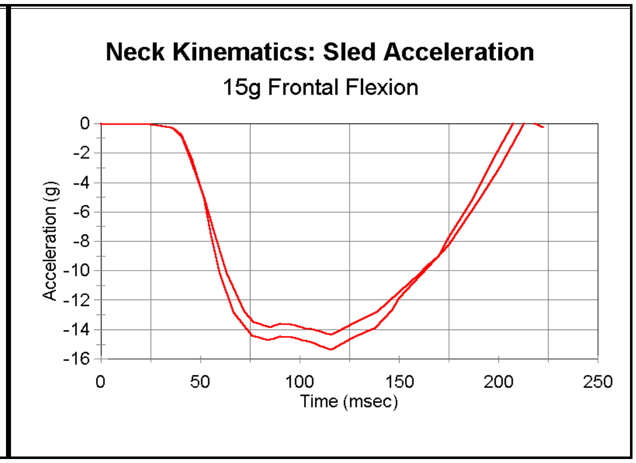


Figure 3. Input sled acceleration for volunteers for 15 G frontal flexion test of neck.

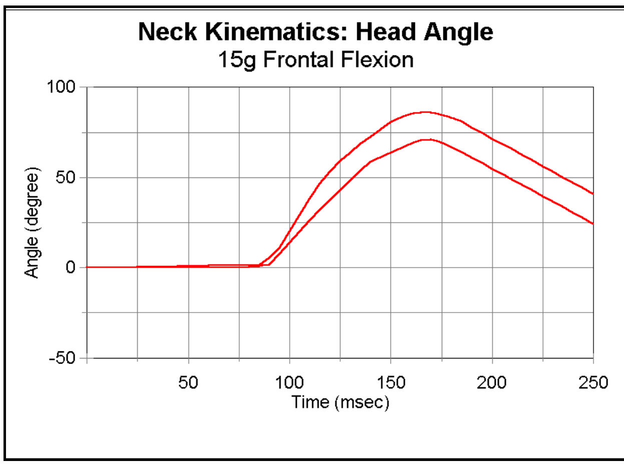


Figure 4. Head rotation angle corridor for 15 G frontal flexion test.

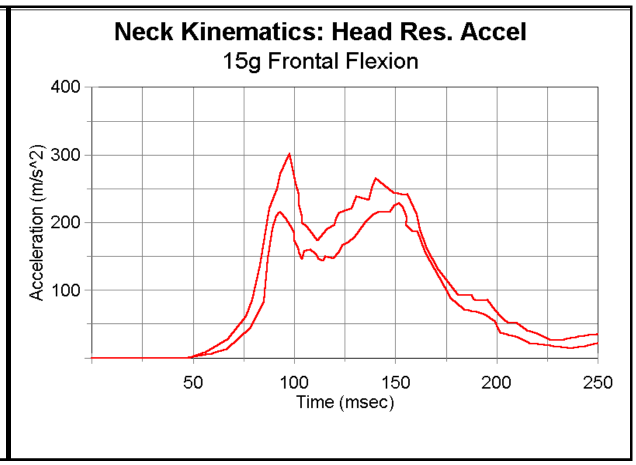


Figure 5. Corridor for resultant acceleration of head C.G. for 15 G frontal flexion test.

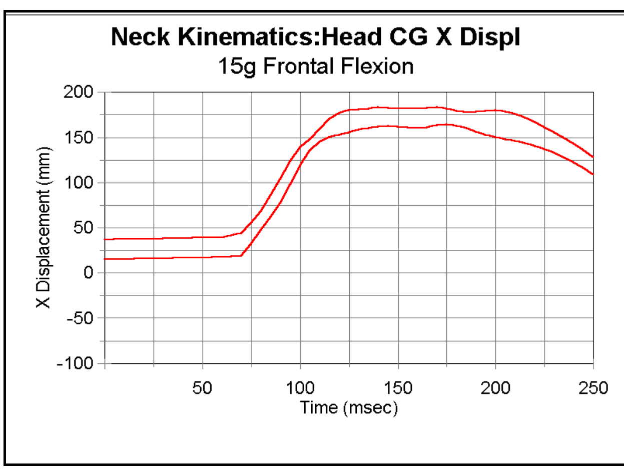


Figure 6. Head C.G. X displacement corridor for 15 G frontal flexion test.

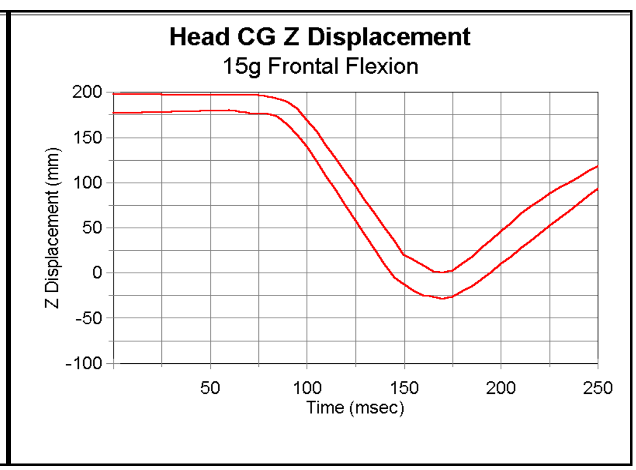


Figure 7. Head C.G. Z displacement corridor for 15 frontal flexion test.

As indicated above, the dynamic response of the neck for frontal flexion is defined by the corridors presented by Mertz and Patrick [1971]. The moment is measured about the occipital condyle, and the angle measures the angle of the head relative to the torso (with respect to the neutral head position). The frontal flexion corridor will implicitly contain the contribution from any chin-chest contact which accounts for the large increase of the moments at the higher angles. Figure 8 shows the moment-angle corridor for flexion.

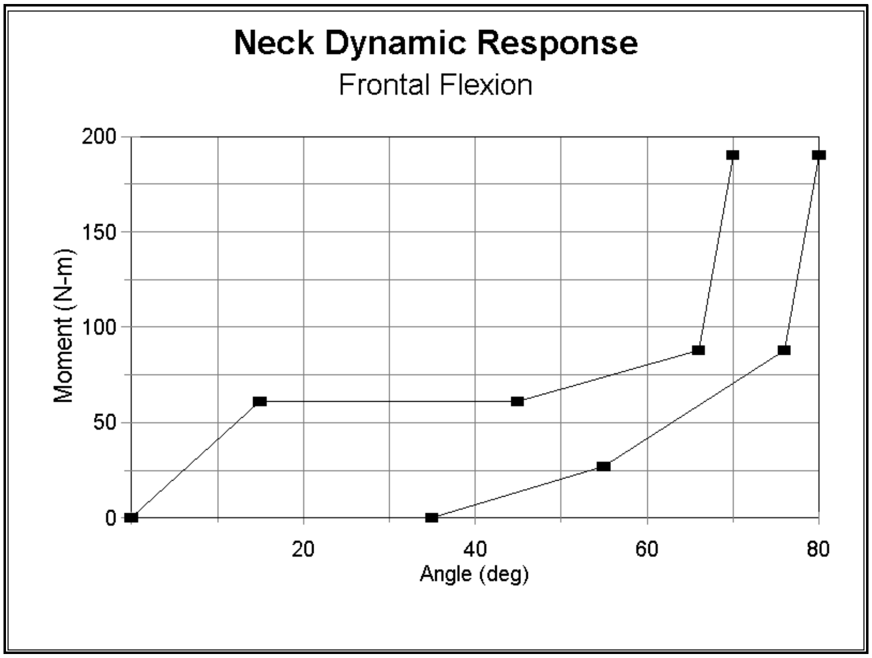


**Figure 8. Moment-angle corridor for frontal flexion, measured at occipital condyle.**

## 3.2 Neck Kinematic and Dynamic Requirements in Lateral Flexion

### Description

The lateral flexion requirements are based on the same NBDL studies listed in section 2.2.1. For these requirements, the data presented by Klinich [1995] are used.

In the Klinich study, the corridors for the head and neck angles were provided. An approximation to the head C.G. displacement corridors were obtained in the following way:

The neck and head anthropometry provided in the paper by Klinich, was used to determine the vector location of the occipital condyle (O.C.) relative to T1 and the location of the head C.G. relative to the O.C. The location of the principal landmarks (in meters) used were:

| | | |
|---|---|---|
| T1: | x = 0.; | z = 0. |
| O.C.: | x = -.003; | z = .119 |
| Head C.G.: | x = .014; | z = .058 |

These measurements were made with the head and neck aligned. The standard deviation in the head and neck angles were then used to determine the relative deviation to be expected in the horizontal and vertical displacements of the head C.G. at each time.

### Test Setup

The setup for this test is given by:

1. The subject is seated on the sled, facing laterally with respect to the sled moving direction.
2. Subjects restrained by pair of shoulder belts, a lap belt, and an inverted-V pelvic strap tied to the lap belt. A 25 cm wide chest strap is used to minimize the load on the right shoulder. In addition, a lightly padded wooden board is placed against the right shoulder to limit the upper torso motion.
3. The motion of the sled is adjusted to have a acceleration curve shown as Figure 9.
4. Use target marks and accelerometers to record the kinematic and dynamic responses of the subject.

For testing the biofidelity of the Thor neck in lateral flexion, the procedure is simplified by testing the head and neck assembly only, with the base of the neck being directly attached to a sled apparatus (optionally through a lower neck load cell) that can duplicate the acceleration pulse seen at the T1 location. There will be some discrepancy with the whole-body test, since the rotation at T1, which may occur in the volunteer testing, cannot be generated with this procedure.

### Biomechanical Requirement

The input acceleration pulse at T1 is shown in Figure 9 and the original sled pulse is shown in Figure 10 for reference. The responses for the 15 G frontal flexion test are shown in Figures 11 to 13.

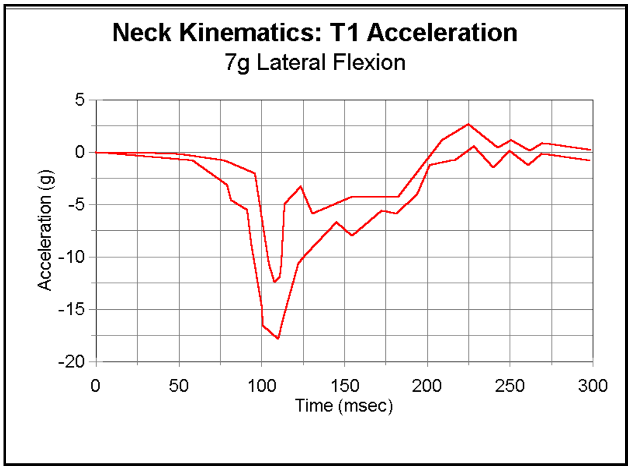


**Figure 9. Input acceleration pulse for 7 G lateral flexion test of neck (equivalent to T1 acceleration of volunteers).**

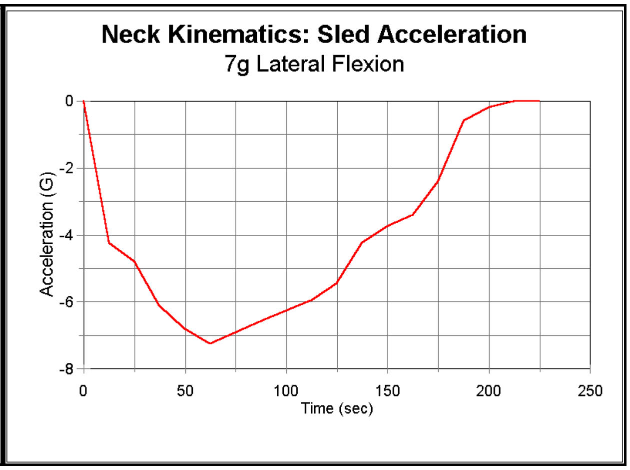


**Figure 10. Input acceleration for 7G neck lateral flexion test**

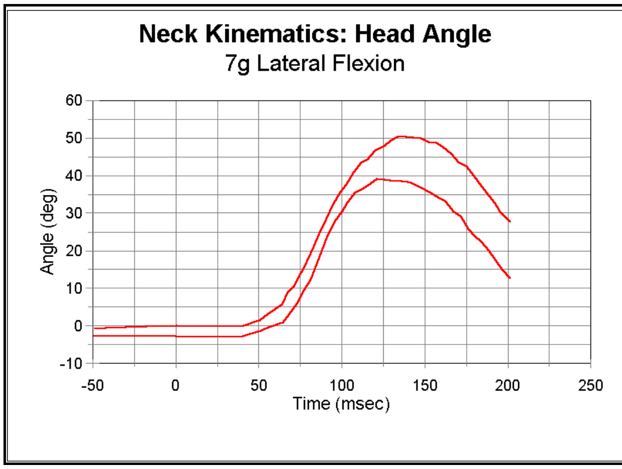


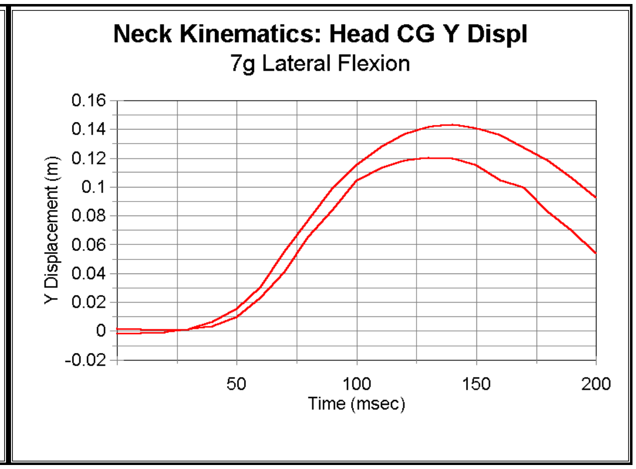


**Figure 11. Head angle rotation corridor for 7 G lateral flexion test.**

**Figure 12. Head CG Y displacement corridor for 7 G lateral flexion test.**

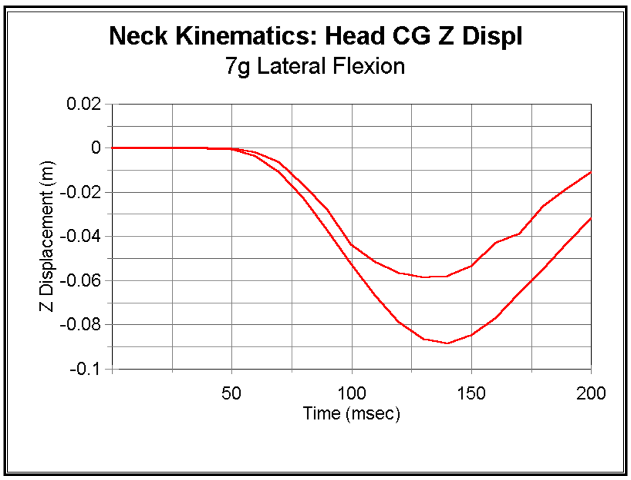


**Figure 13. Head CG Z displacement corridor for 7 G lateral flexion test.**

The dynamic response of the neck for lateral flexion is defined by the corridors presented by Patrick and Chou [1971]. Figure 13 shows the moment-angle corridor for the neck moment at the O.C. during lateral flexion.

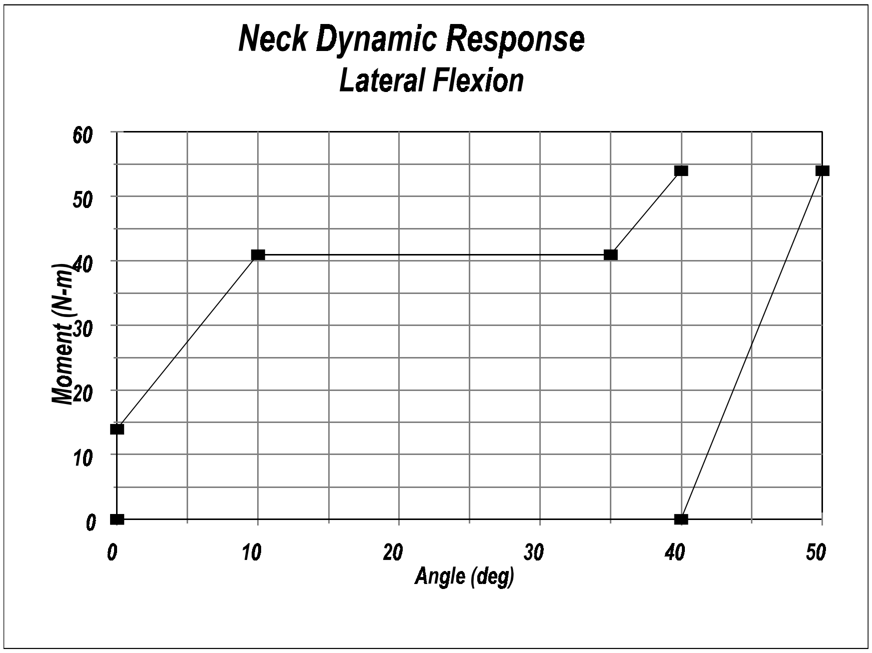


**Figure 14. Moment-angle corridor measured at occipital condyle for lateral flexion**

# 4. THORAX

## 4.1 Sternal Impact

**References**

Neathery, R. 1974. *Analysis of Chest Impact Response Data and Scaled Performance Recommendations.* Proceedings of the 18th Stapp Car Crash Conference.

**Description**

The principal response corridors for sternal impact are the traditional Kroell corridors for rigid disk impacts at 6.7 m/s and 4.3 m/s at the upper ribcage. The normalized curves provided by Neathery [1974] define the appropriate response requirements for this type of impacts for a 50th percentile U.S. male.

**Test Setup**

The test configuration for performing the Kroell tests consists of:

1. A rigid and flat impactor with a 152 mm diameter and mass of 23.4 kg.
2. The subject is set up in a sitting position, with no back support and its legs horizontal and the arms raised.
3. The subject is positioned in front of impactor such that the center line of the impactor is at the middle of ribs 4 and 5, near the mid-line of the sternum.
4. Two impact speeds are tested: one at 6.7 m/s and one at 4.3 m/s.
5. The force-deflection characteristics are obtained from the test, including the unloading portion of the force to estimate the amount of hysteresis.

**Biomechanical Response**

The sternal impact response is defined by the following two corridors representing the response at the two impact speeds:

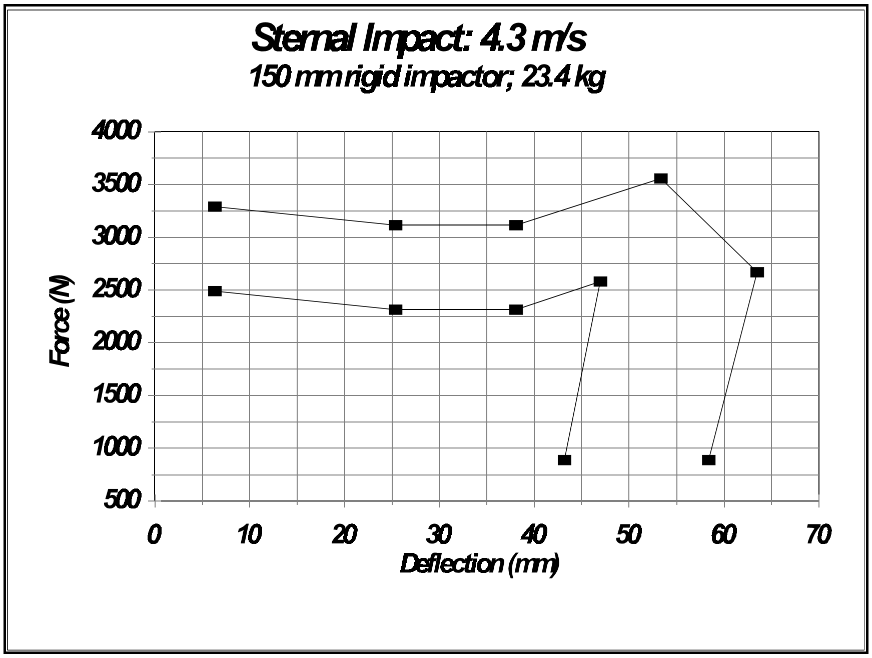


**Figure 15. Force-deflection response of thorax for central disk impact at 4.3 m/s**

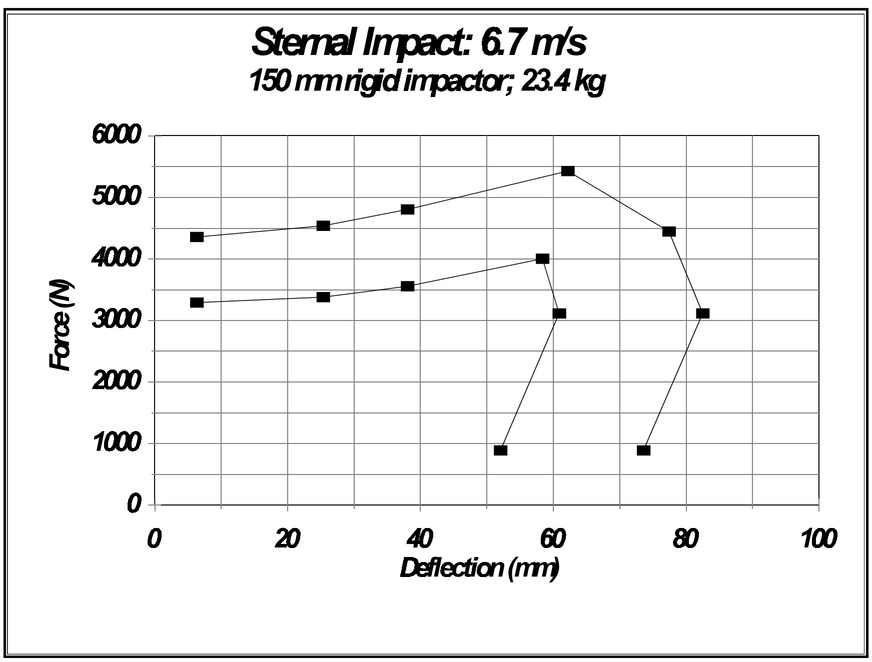


**Figure 16. Force-deflection response of thorax for central disk impact at 6.7 m/s.**

### 4.2 Lower Ribcage Oblique Impact

**References**

Yoganandan, N., Pintar, F., Kumaresan, S., Haffner, M., Kuppa, S. 1997. *Impact biomechanics of the human thorax-abdomen complex*. International Journal of Crash, Vol 2, No. 2, pp 219-228

**Description**

This test is based on oblique impacts at the lower ribcage performed by Medical College of Wisconsin (MCW) [Yoganandan, 1997]. In these tests, the torso was initially rotated from right to left by 15°, such that the impact occurred on the right antero-lateral thorax. The instrumentation in the MCW tests consisted of a load cell and uniaxial accelerometer attached to the pendulum to measure the impact forces. The chest deflection was measured with a chest band which measured the external deformation of the thorax. The response characteristics of the lower ribcage are shown as a force-time corridor, a deflection-time corridor and a combined force-deflection corridor.

**Test Setup**

The test configuration for performing the MCW test consists of:

1. The lower extremities are stretched horizontally and the upper extremities are extended forward to allow positioning of the torso. The back of the torso was unsupported.
2. Impactor consisted of a 150 mm diameter rigid disk with a mass of 23.4 kg. The face of the impactor was covered with a Rubatex R-451N padding of thickness 19 mm. The padding was rectangular in shape with each edge 150mm in length. The padding characteristics are shown below.

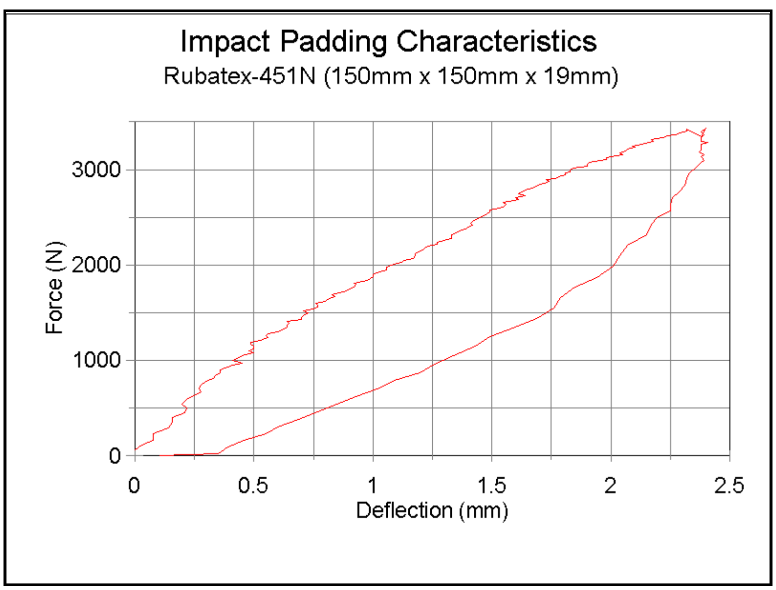


**Figure 17. Force-deflections characteristics of padding used in oblique impacts of lower ribcage.**

3. Long underwear was placed on the subject to provide realistic seat interaction.
4. The subject was seated facing the impactor on a thin teflon sheet.
5. The legs and arms were fully extended and the subject was seated on a low friction surface.
6. The impact velocity was 4.3 m/s.

**Biomechanical Response**

There are three responses that are used to define the overall lower ribcage response to oblique impact. These are the force-deflection response, the force time history, and the deflection time history. These are shown in Figures 18-20. The primary requirement will be to meet the force-deflection response.

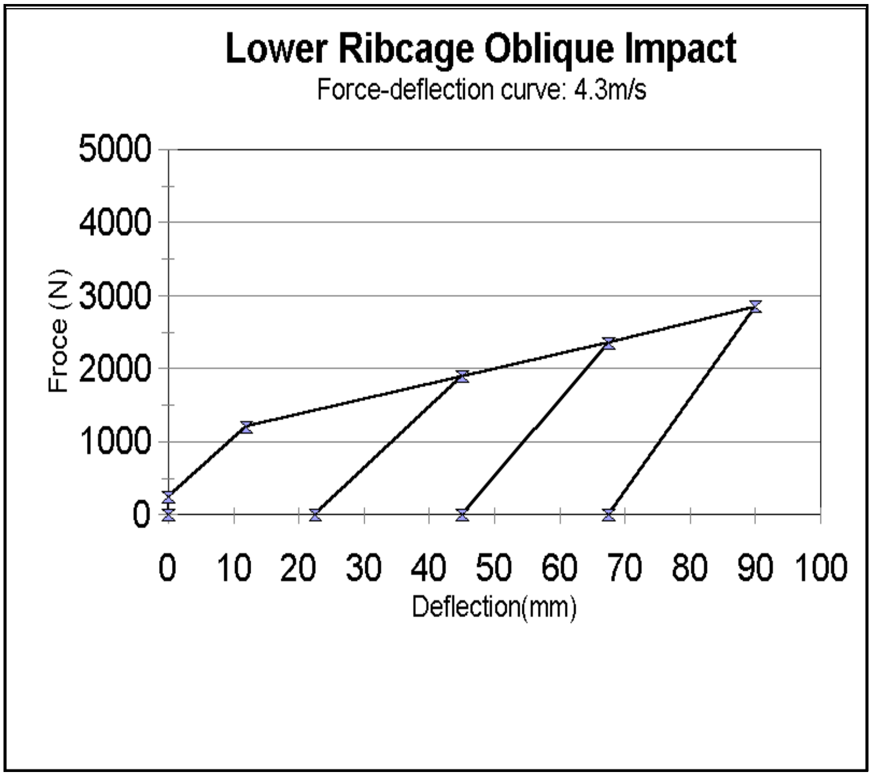


**Figure 18. Force-deflection response for lower ribcage/abdomen oblique impacts at 4.3 m/s.**

The above figure shows the average force-deflection curve along with the lower and upper corridors for the force-deflection response (at ± 1 std dev). All three curves have the same loading slope and approximately the same unloading slopes but different peak force and deflection values.

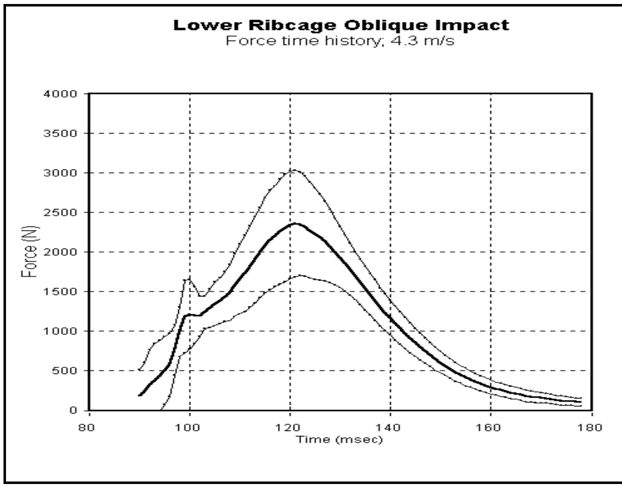


Figure 19. Force-deflection response for lower ribcage/abdomen oblique impacts at 4.3 m/s.

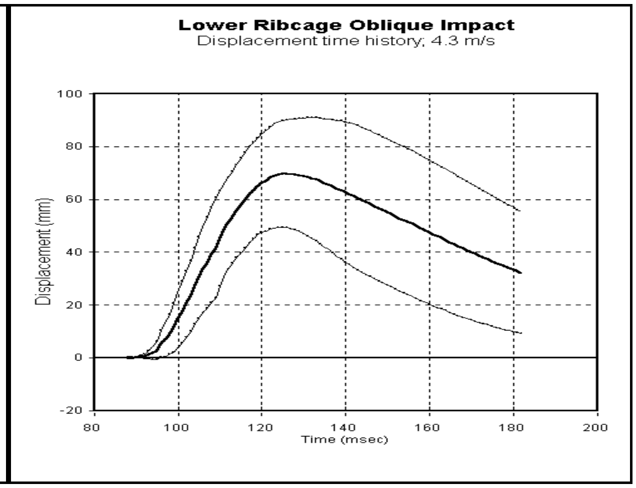


Figure 20. Deflection-time response for lower ribcage/abdomen oblique impacts at 4.3 m/s.

# 5. ABDOMEN

## 5.1 Upper Abdomen: Steering Wheel Impact

### References

Nusholtz, G., and Kaiker, P. 1994. *Abdominal Response to Steering Wheel Loading.* Proceedings of the 14th International Conference on Experimental Safety Vehicles.

### Description

The response requirement for upper abdomen impact is derived from data developed by Nusholtz [1994] based on steering wheel impacts with engagement at region of L2. Six tests were performed with impact speeds of 3.9 m/s to 10.8 m/s with an average speed of 8.0 m/s. There is increasing stiffness seen after a penetration of 80 mm, which probably arises from engagement of the steering wheel with the lower ribcage structure.

### Test set-up

The test configuration for performing the upper abdomen impact test consists of:

1. Impactor consists of 18 kg rigid steering wheel, rigidly mounted at an angle of 45°.
2. The subject is set up in a sitting position, with no back support and its legs and the arms raised (may be taped lightly to a support bar).
3. The lower thoracic spine is maintained in a vertical position and the leading edge of the steering wheel should be at the level of upper abdomen.
4. The impact speed should be 8.0 m/s.
5. Impactor force should be obtained and the external penetration obtained using a linear displacement transducer.

### Biomechanical Response

The force vs. penetration corridor is given in Figure 21.

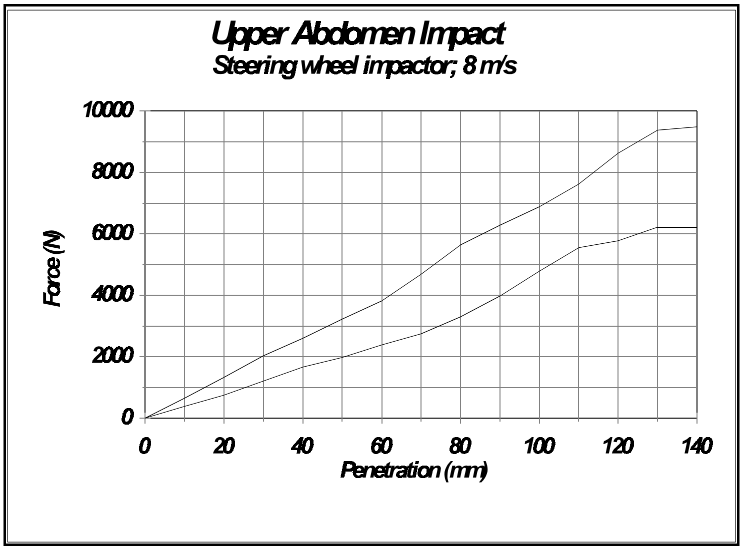


**Figure 21. Force-penetration response for upper abdomen to rigid steering wheel impact at 8.0 m/s.**

## 5.2 Lower Abdomen: Rigid Rod Impact

### References

Cavanaugh, J., Nyquist, G., Goldberg, S., and King, A. 1986. *Lower Abdominal Tolerance and Response.* Proceedings of the 30th Stapp Car Crash Conference.

### Description

The response requirement for lower abdomen impact have been derived from the low severity tests performed by Cavanaugh [1986]. The requirement is in the form of a force vs external penetration corridor. The tests were conducted using a 25 mm diameter rigid bar of length 30 cm and mass 32 kg, impacting perpendicularly the abdomen of cadavers at vertical location of approximately L3. Five tests were performed in the speed range of 4.9 to 7.2 m/s with an average impact speed of 6.1 m/s.

### Test Setup

The test configuration for performing the abdomen impact test consists of:

1. Impactor is a 25 mm diameter, 30 cm long rigid cylindrical rod with mass of 32 kg
2. The dummy is set up in a sitting position, with no back support and its legs horizontal and the arms raised (may be taped lightly to a support bar).
3. The lower thoracic spine is maintained in a vertical position and the center line of the impactor was approximately at the level of L2.
4. The average impact speed was 6.1 m/s (for the low velocity impacts).

## Biomechanical Response

The force vs. penetration corridor is given in Figure 22.

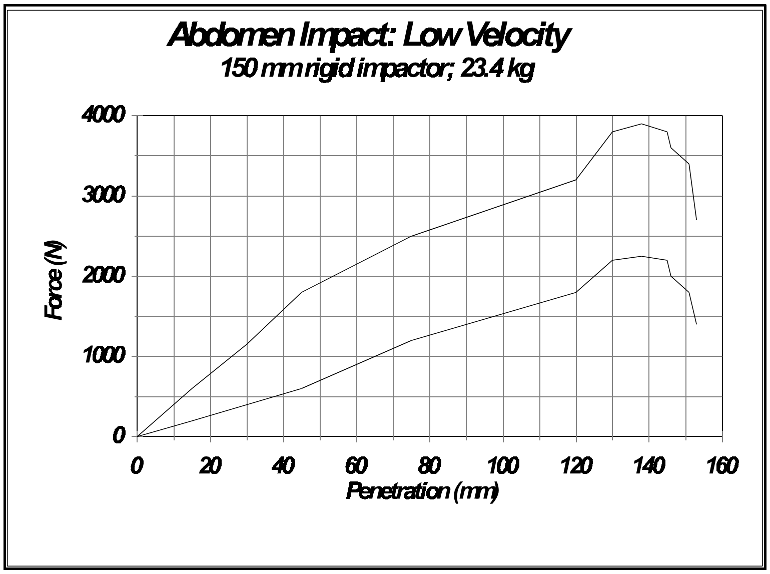


**Figure 22. Force-penetration response for lower abdomen impact with rigid rod at 6.1 m/s.**

## 6. FEMUR

### References

Horsch, J., and Patrick, L. 1976. *Cadaver and Dummy Knee Impact Response.* Proceedings of the 20th Stapp Car Crash Conference. SAE Paper # 760799.

### Description

This requirement defines the response of the femur to axial impacts at the knee. The responses are based on the tests and analysis of Horsch and Patrick [1976]. They conducted knee impacts along the femoral axis of unembalmed male cadavers with a rigid pendulum impactor. Only the whole body impact tests are used for defining the requirement.

The primary requirements define the peak knee impact forces generated when impactors of different masses with different impact speeds are allowed to impact the knee. Horsch and Patrick expressed the combined effect of both mass and speed by using a single variable which was proportional to the initial energy of the impactor system. The impactors were a series of flat faced, rigid pendulum impactors. Their face diameters varied between 38 mm to 152 mm and their weights varied between .24 kg to 25 kg. The tests using the 25 kg impactors are not included in the requirement definition since these were far larger than any of the other impactor sizes used. The pendulums were dropped from heights of .1 m to .8 m. corresponding to impact speeds of 1.4 m/s to 4.0 m/s.

### Test Setup

The test configuration for performing the femur impact test consists of:

1. Impactor is a 75 mm diameter, rigid, flat faced with mass of 5 kg
2. The subject was seated on a flat seat with no back support with the lower leg hanging over the seat edge and the feet resting lightly on the floor. The lower leg made an angle between 90° - 105° relative to the femur.
3. the left or right knee was placed such that the center of the knee was in line with the axis of the impactor and this axis was approximately in line with the femur axis.
4. Tests are conducted at two impact speeds: namely 2.0 m/s and 3.0 m/s
5. Measurements include the impact force on the knee as measured by the impactor and the acceleration along the axis of the femur as measured by an accelerometer placed proximal to the knee.

### Knee Impact Calculation Procedure

The single independent variable defined by Horsch and Patrick which is a function of drop height and reduced mass was based on a two mass model of the impactor and the subject knee. The effective subject mass is determined by them by fitting a straight line to the force vs acceleration curve generated from the knee impact. Thus:

$$F_{knee} = m_s . a_{leg}$$

where: $F_{knee}$ = impact force measured at knee
$a_{leg}$ = acceleration measured on leg
$m_s$ = effective subject mass

With this value of effective mass, a new independent variable is defined:

$$E_e = h.\ m_p\, m_s/(m_p + m_s)$$

where: $h$ = drop height of pendulum = $v^2/2g$ (v = impact speed)
$m_p$ = mass of pendulum

This variable will be termed the effective impact energy. The term $m_p\, m_s/(m_p + m_s)$ is the reduced mass of the two mass system. For the rigid mount case, the subject mass is very large and the reduced mass is effectively equal to $m_p$. For the whole body case, the acceleration time history of the proximal femur is used to determine the effective femur mass which should be used in the calculation of the effective impact energy described above. During the period when the knee is being loaded by the impactor, the impact is approximated by the two mass system (impactor and femur). The effective femur mass is determined from a regression fit to the equation: $F_{fem} = m_{fem}a_{fem}$

**Biomechanical Response**

The knee impact response for the whole body configuration is given by Figure 23.

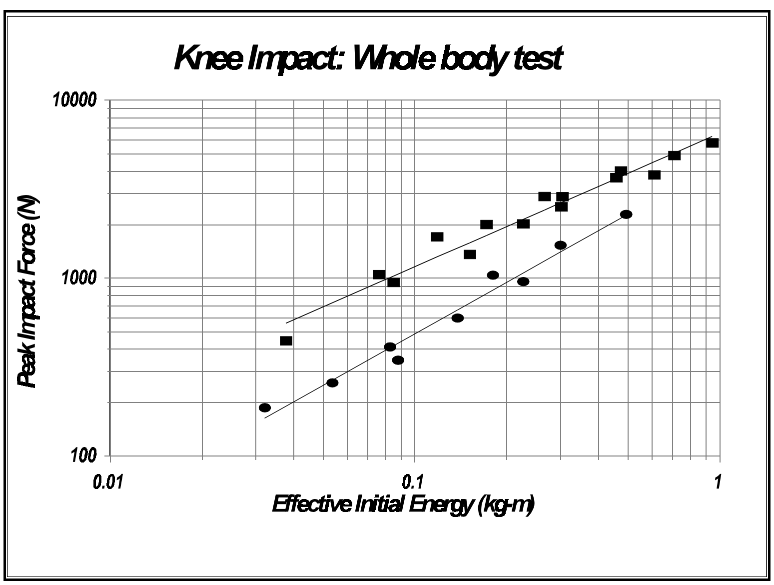


**Figure 23. Knee impact response in whole body configuration for varying impactor mass and velocity.**

# 7. FACE

## 7.1 Rigid Bar Impact

### References

Allsop, D., Warner, C., Wille, M., Schneider, D., and Nahum, A. 1988. *Facial Impact Response - A Comparison of the Hybrid III Dummy and Human Cadaver.* Proceedings of the 32nd Stapp Car Crash Conference.
Melvin, J., and Shee, T. 1989. *Facial Injury Assessment Techniques.* Proceedings of the 12th International Conference on Experimental Safety Vehicles.
Nyquist, G., Cavanaugh, J., Goldberg, S., and King, A. 1986. *Facial Impact Tolerance and Response.* Proceedings of the 30th Stapp Car Crash Conference.

### Description

The facial impact response here is based on rod impacts performed by Nyquist, et al. [1986], Allsop, et al. [1988], and Melvin and Shee [1989]. The response requirements are in the form of force vs time and force vs deflection curves for the rod impact. The response requirements have been summarized by Melvin [1989].

The requirement defines the approximate force-deflection behavior of the face upon impact with a rigid rod. The Nyquist tests used a 25 mm diameter rod, with an attached mass of 32 kg or 64 kg which impacted the faces of unembalmed cadavers across the nose and zygoma. The average contact velocity for the tests was 3.6 m/s (with a range of 2.8 to 4.8 m/s). The Allsop tests used a 20 mm diameter bar composed of semi-circular disks. The impact mass was 14.5 kg and was dropped from heights of 305 to 610 mm (corresponding to impact speeds of 2.45 to 3.46 m/s). Impacts were conducted on the zygoma and the maxilla.

The critical force part of the above force-deflection curve is the portion between about 12 mm and 25 mm. The region before this, as indicated by Melvin, indicates the response of the facial skin and other soft tissue and can be highly variable. The steeper section of the curve corresponds to the loading of the facial skeletal structure.

### Test set-up

For the rod impact test to the face, the configuration is defined as:

1. The torso of the subject is maintained straight and the head vertical, with the legs kept horizontal and arms raised.
2. The rod and impactor assembly will have a total mass of 32 kg.
3. The impact speed is set to 3.6 m/s (average of the range 2.4 - 4.8 m/s in cadaver testing).
4. The rod is configured to impact along the mid-line of the left and right maxilla plates on face.

**Biomechanical Response**

The force vs time response for impact by a rigid bar across the zygomatic region with impact speeds between 2.8 m/s and 4.8 m/s is given by the following figure. (The figure below was based solely on the data presented by Nyquist, since Allsop did not present force vs time curves.)

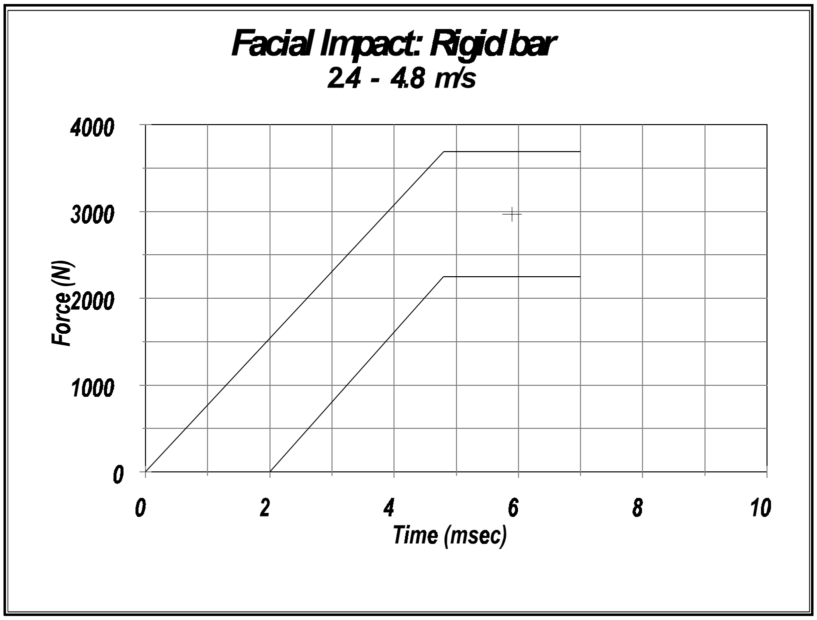


**Figure 24. Force-time response for facial impact with rigid rod to zygomatic region.**

## 7.2 Disk Impact

**References**


Allsop, D., Warner, C., Wille, M., Schneider, D., and Nahum, A. 1988. *Facial Impact Response - A Comparison of the Hybrid III Dummy and Human Cadaver.* Proceedings of the 32nd Stapp Car Crash Conference.

Melvin, J., and Shee, T. 1989. *Facial Injury Assessment Techniques.* Proceedings of the 12th International Conference on Experimental Safety Vehicles.

Nyquist, G., Cavanaugh, J., Goldberg, S., and King, A. 1986. *Facial Impact Tolerance and Response.* Proceedings of the 30th Stapp Car Crash Conference.


**Description**

The facial impact response here is based on disk impacts performed by Nyquist, et al. [1986], Allsop, et al. [1988], and Melvin and Shee [1989]. The response requirement is in the form of force vs time curve for the disk impacts. The response requirements have been summarized by Melvin [1989].

**Test set-up**

For the disk impact, the configuration is defined as:

1. The torso of the subject is maintained straight and the head vertical, with the legs kept horizontal and arms raised.
2. The disk and impactor assembly will have a total mass of 13 kg.
3. The impact speed is set to 6.7 m/s.
4. The center of the disk is configured to impact at the mid-point of the line joining the two maxilla plates on the face.

**Biomechanical Response**

The force vs time response for distributed loading due to a 152 mm diameter disk is given by Figure 25.

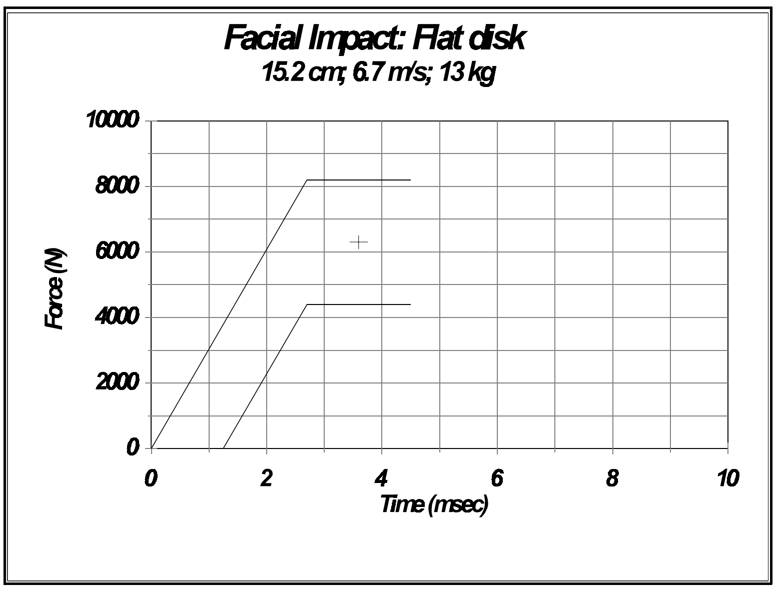


**Figure 25. Force-time response of facial impact by disk.**

# 8. LOWER LEG/ANKLE/FOOT

## 8.1 Dynamic Heel Impact

### References

Kuppa, S., Klopp, G., Crandall, J., et al. 1998. *Axial Impact Characteristics of Dummy and Cadaver Lower Limbs.* 16th International Technical Conference on the Enhanced Safety of Vehicles. Vol. 2, pp 1608-1617.

### Description

The response of the lower leg to impact on the plantar surface of the foot is based on the tests conducted at the Medical College of Wisconsin [Kuppa, 1998]. In these tests the rotation of the foot was minimized. The lower limb was amputated at the knee and attached to a mini-sled with the total mass of 16.8 kg. A pendulum of mass 23.5 kg was used to the impact the plantar surface of the foot. The mini-sled was free to move on the rails after impact. Tests were conducted with impact speeds from 2.2 m/s to 5.6 m/s.

### Test Setup

For the axial impact along the lower leg, the configuration is defined as:

- The lower leg specimen (with foot) was rigidly attached at the proximal tibia to a minisled of total mass 16.8 kg. The sled was allowed to move freely on horizontal rails.
- The plantar surface of foot was impacted with a 23.5 kg impactor with impact speeds in the range of 2.2 m/s to 5.6 m/s.
- Impact force at the heel and force at the proximal tibia were measured.

### Biomechanical Response

The biomechanical response is defined by the peak impact force seen for each impact velocity. This is plotted in the following graph.

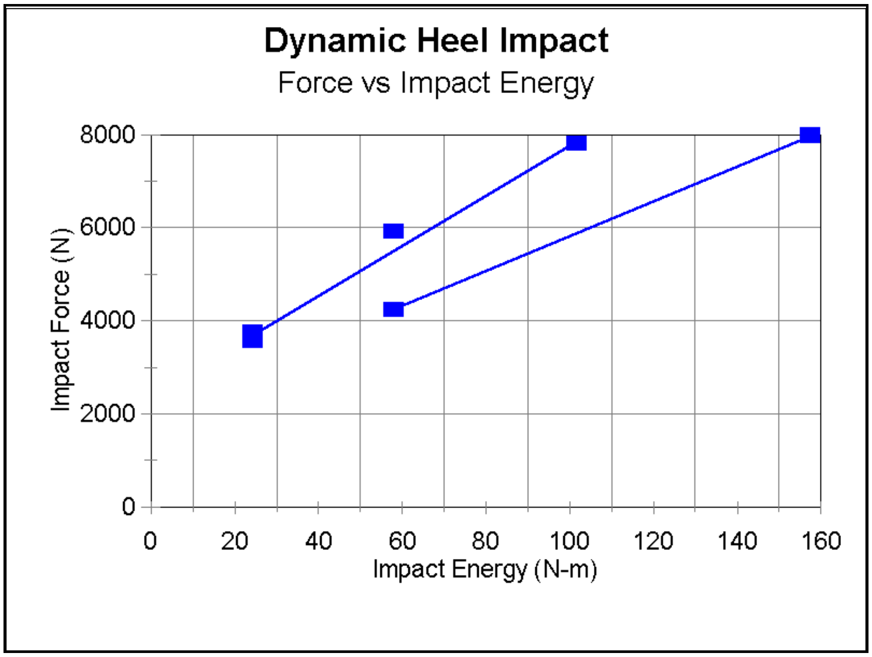


**Figure 26. Peak force response for axial impacts through heel with varying impact energies.**

## 8.2 Dynamic Dorsiflexion

### References

Crandall, J., Portier, L., Petit, P., et al. 1996. *Biomechanical Response and Physical Properties of the Leg, Foot, and Ankle.* Proc. 40th Stapp Car Crash Conf., SAE Paper No. 962424, pp 173-192.

### Description

The dynamic dorsiflexion response is given by the moment vs. angle characteristics at the ankle, when the ball of the foot is impacted . The response was obtained from cadaver tests conducted at Renault [Crandall, 1996; Portier, 1997]. Only the data during loading were considered, since, in addition to dorsiflexion, the foot would tend to invert or evert during the unloading phase. The data are derived from the right and left legs of only one subject.

### Test Setup

1. Foot set at about 90 deg relative to tibia.
2. Impact ball of foot at 5 m/s.
3. Measure forces and moments at distal tibia and compute moment at ankle, moment through the ankle cross-section, and the Achilles tension force.

## Biomechanical Response

The moment-angle response corridor estimated from the cadaver tests is shown in the following graph.

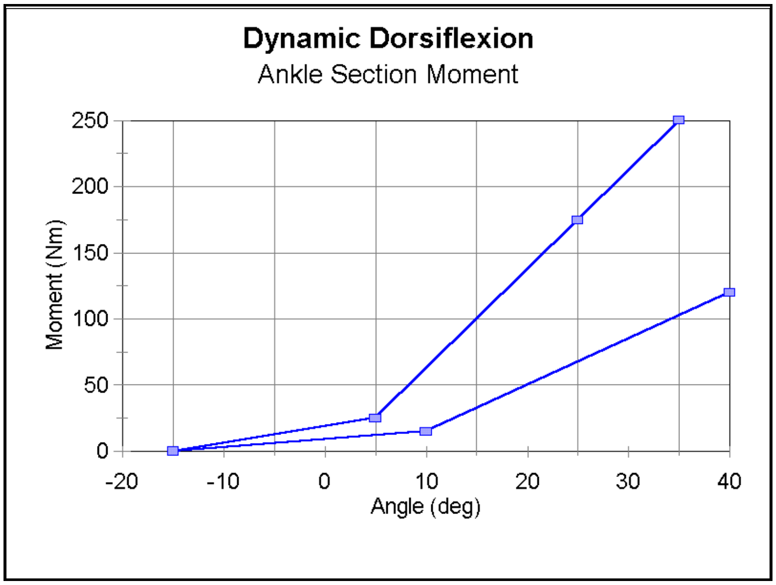


**Figure 27. Moment-angle response for total ankle section in dynamic dorsiflexion**

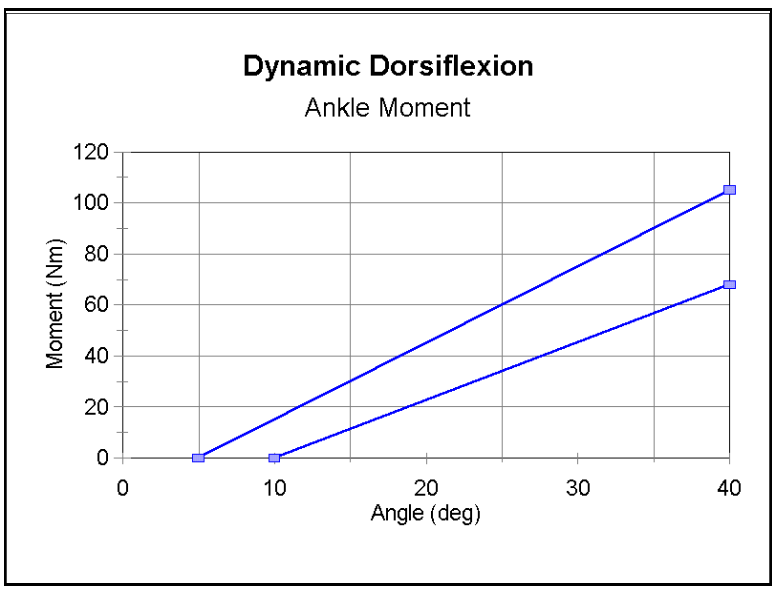


**Figure 28. Moment-angle response at ankle only in dynamic dorsiflexion.**

## 8.3 Quasi-static Inversion

### References

Crandall, J., Portier, L., Petit, P., et al. 1996. *Biomechanical Response and Physical Properties of the Leg, Foot, and Ankle.* Proc. 40th Stapp Car Crash Conf., SAE Paper No. 962424, pp 173-192.

Petit, P., et al. 1996. *Quasi-static Characterization of the Human Foot-Ankle Joints in a Simulated Tensed State and Updated Accidentological Data.* Proc. of the 1996 IRCOBI Conference.

### Description

Quasi-static moment vs angle response when the foot is rotated in inversion was obtained from tests conducted by Renault [Petit, 1996]. Similar tests were conducted with human volunteers by University of Virginia [Crandall, 1996]. In the Renault tests, the cadaver legs were amputated 15 cm above the malleoli and the proximal ends of the tibia and fibula were fixed in bone cement. Rotation of the foot was accomplished by applying a torque to the calcaneous through a shaft attached to it. The rotations in the UVa tests were performed using a special six degree-of-freedom fixture that allows rigid rotations of the foot relative to the tibia along any specified axis. The proposed requirement is based, currently, on the Renault data, since the UVa volunteer showed fairly large maximum inversion angles (greater than 50 degrees), which may not be realistic.

### Test Setup

1. Set foot at 90° with respect to the tibia.
2. With the tibia held fixed, apply a moment to rotate the foot in inversion. The moment can be applied using an external force acting at the end of the foot.
3. Measure moment at ankle (using lower tibia load cell or external load cell) and angle of rotation.

### Biomechanical Response

The moment-angle response for quasi-static inversion is given by the following graph. This is derived from the data from the Renault cadaveric tests.

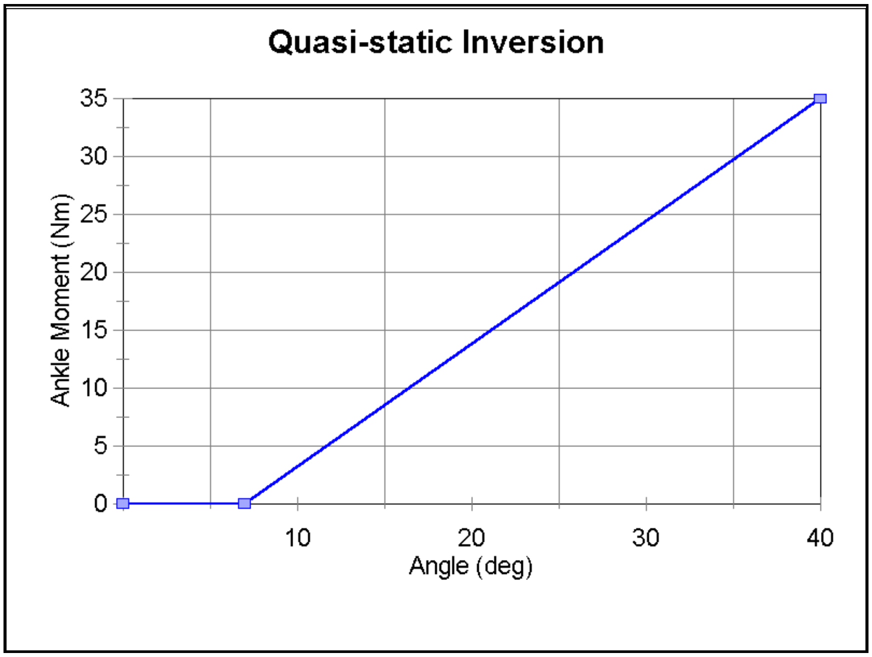


**Figure 29. Moment-angle response for quasi-static inversion.**

## 8.4 Quasi-static Eversion

### References

Crandall, J., Portier, L., Petit, P., et al. 1996. *Biomechanical Response and Physical Properties of the Leg, Foot, and Ankle.* Proc. 40th Stapp Car Crash Conf., SAE Paper No. 962424, pp 173-192.

Petit, P., et al. 1996. *Quasi-static Characterization of the Human Foot-Ankle Joints in a Simulated Tensed State and Updated Accidentological Data.* Proc. of the 1996 IRCOBI Conference.

### Description

Quasi-static moment vs. angle responses in eversion were obtained from tests conducted by Renault [Petit, 1996] using cadaveric subjects and by UVa using volunteers [Crandall, 1996]. The procedures are described in the previous section on the quasi-static inversion requirement. The results from both labs are similar and a single moment-angle curve can be derived from both sets of data.

### Test Setup

1. Set foot at 90° with respect to the tibia.
2. With the tibia held fixed, apply a moment to rotate the foot in eversion. The moment can be applied using an external force acting at the end of the foot.

3. Measure moment at ankle (using lower tibia load cell or external load cell) and angle of rotation.

**Biomechanical Response**

The moment-angle response in quasi-static eversion is given by the following graph.

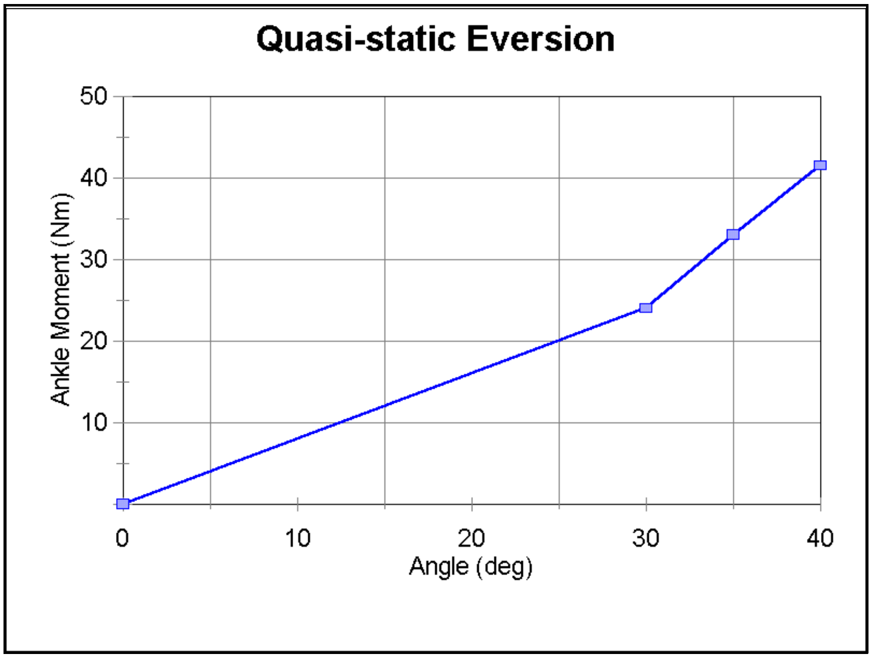


**Figure 30. Moment-angle response for quasi-static eversion.**

## 8.5 Quasi-static Dorsiflexion

**References**

Crandall, J., Portier, L., Petit, P., et al. 1996. *Biomechanical Response and Physical Properties of the Leg, Foot, and Ankle.* Proc. 40th Stapp Car Crash Conf., SAE Paper No. 962424, pp 173-192.

**Description**

University of Virginia performed cadaver and volunteer tests using the test fixture used in the inversion and eversion testing. [Crandall, 1996]. The volunteer tests were conducted with the subjects in a relaxed state. The lower leg was restrained using nylon straps, while the foot was placed in an athletic shoe, which was restrained to a foot plate using straps. Tests were conducted with knee flexion at 0° and 90° .

The lower legs of the cadavers were amputated at the mid-diaphysis of the femur and all the musculature and joints influencing the ankle joints were retained. Knee flexion was maintained at either 0° or 90°. Quasi-static dorsiflexion tests were also performed by Renault. In these tests, the cadaver legs were amputated 15 cm above the malleoli and the proximal ends of the tibia and fibula were fixed in bone cement. Muscle tension of 900 N was simulated by applying a constant tension in the Achilles tendon.

The proposed requirement is based on the volunteer response with the knee flexed at 90°, since probably best imitates the natural state of the ankle in a driving environment.

**Test Setup**

1. Set foot at 90° with respect to the tibia.
2. With the tibia held fixed, apply a moment to rotate the foot in dorsiflexion. The moment can be applied using an external force acting at the end of the foot.
3. Measure moment at ankle (using lower tibia load cell or external load cell) and angle of rotation.

**Biomechanical Response**

The moment vs. angle responses under quasi-static dorsiflexion are given by the following graphs. The first graph shows the response for the complete ankle section, including the effect of the Achilles, while the second graph shows the response only of the ankle joint.

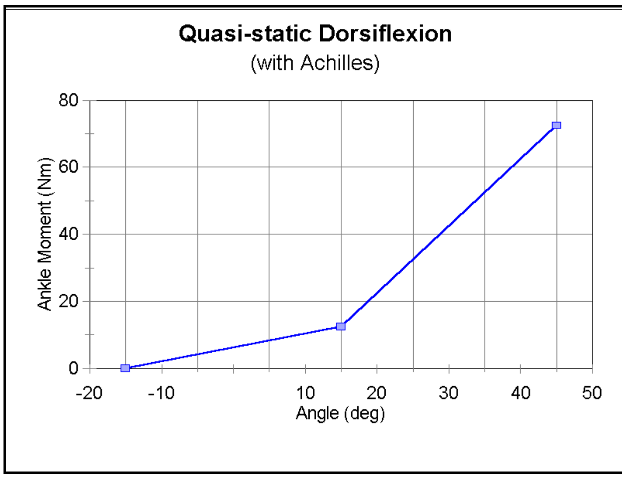


**Figure 31. Moment-angle response for ankle with Achilles, for quasi-static dorsiflexion.**

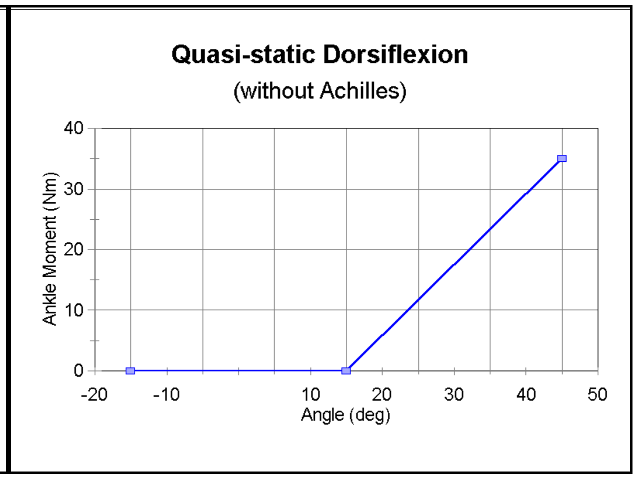


**Figure 32. Moment-angle response for ankle only, for quasi-static dorsiflexion.**

## 8.6 Quasi-static Plantarflexion

**References**


Paranteau, C. et al. 1996. *A New Method to Determine the Biomechanical Properties of Human and Dummy Joints.* Proc. of the 1995 IRCOBI Conference.

**Description**

Paranteau [1996] determined quasi-static plantarflexion response using cadaver lower legs which had been excised at the distal tibia-fibula. The moment-angle response correspond to the effect of the ankle only, since there is no passive response from the musculature of the anterior crural compartment which had been severed. UVa conducted plantarflexion tests with volunteers in a relaxed state. These tests show much higher responses than the Paranteau tests. The likely reason is the effect of the passive and active muscles in the volunteer response. The data also indicated that there was no or very low moment for the first 25°. The proposed requirement will use the Paranteau data, with an initial flat response up to 25°.

**Test Setup**

1. Set foot at 90° with respect to the tibia.
2. With the tibia held fixed, apply a moment to rotate the foot in plantarflexion. The moment can be applied using an external force acting at the end of the foot.
3. Measure moment at ankle (using lower tibia load cell or external load cell) and angle of rotation.

**Biomechanical Response**

The moment vs. angle response in quasi-static plantarflexion is given by the following graph.

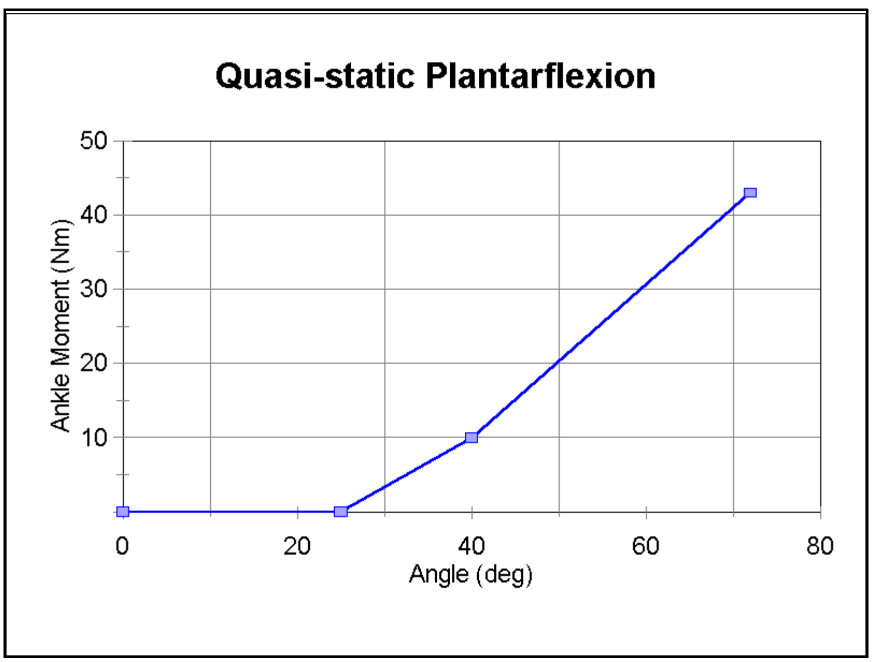


**Figure 33. Moment vs. angle response for quasi-static plantarflexion.**

## 8.7 Quasi-static Internal/External Rotation

### References

Siegler, S., et al. 1988. *The Three-Dimensional Kinematics and Flexibility Characteristics of the Human Ankle and Subtalar Joints - Part I: Kinematics.* Transactions of the ASME, Vol 110.

### Description

The quasi-static response in internal and external rotation is derived from tests performed by Siegler [1988]. This response is not a requirement in the ankle design of Thor, but used as a guide to provide a smooth response when the foot is rotated about the Z-axis (instead of a zero moment response up to the point of contact and a sharp and high response beyond that).

### Test Setup

1. Set foot at 90° with respect to the tibia.
2. With the tibia held fixed, apply a moment to rotate the foot in internal and external rotation.
3. Measure moment at ankle (using external load cell) and angle of rotation.

### Biomechanical Response

The moment vs. angle response is provided by the following graph:

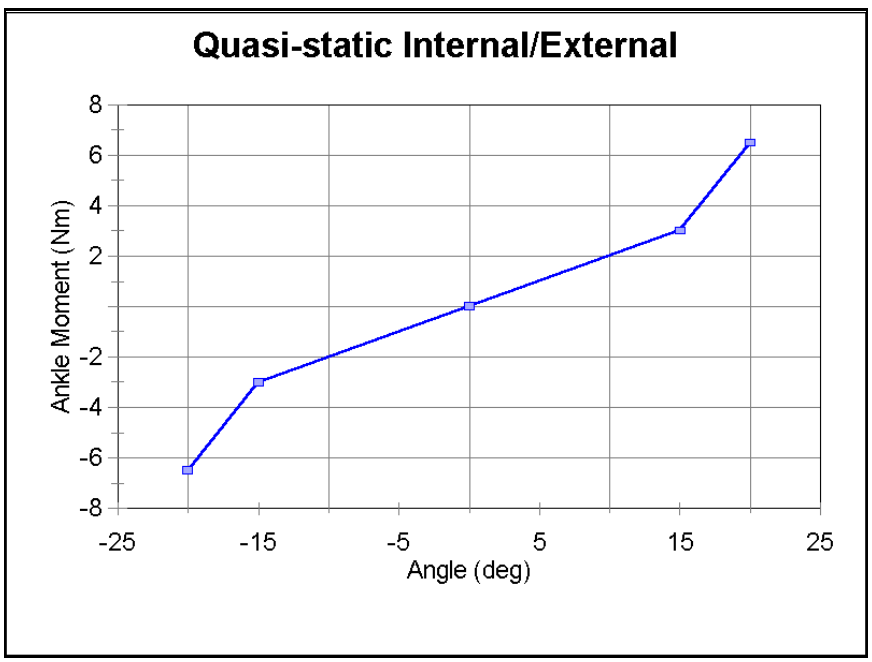


**Figure 34. Moment vs. angle response in quasi-static internal and external rotation.**

## SECTION II. BIOFIDELITY PERFORMANCE OF THOR

### 9. HEAD BIOFIDELITY

The Thor forehead was impacted according to the setup described in Section 2. Both the time to reach peak impact force, and the magnitude of the peak force is within the corridors established for the impact. The peak force is at the lower end of the corridor, perhaps reflecting the fact that part of the impacting surface of the 150mm disk will engage the softer face skin.

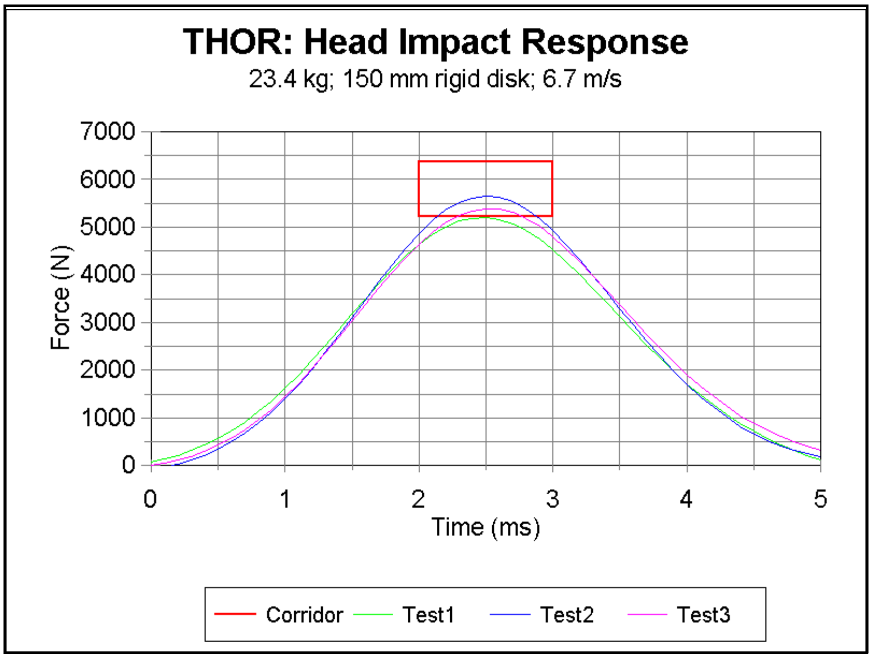


**Figure 35. Response of Thor to forehead impact by 23.4 kg impactor at 2 m/s.**

### 10. NECK BIOFIDELITY

The neck biofidelity was evaluated in testing at several laboratories using a head and neck assembly attached to a HyGe sled. As indicated in Section 3, applying an accerelation to the base of the neck equivalent to the measured T1 acceleration in human volunteer tests, is a reasonable simulation of the whole body tests.

#### 10.1 Frontal Flexion

The following are results obtained from testing at TNO equivalent to the 15 G frontal flexion sled tests carried out on NBDL volunteers.

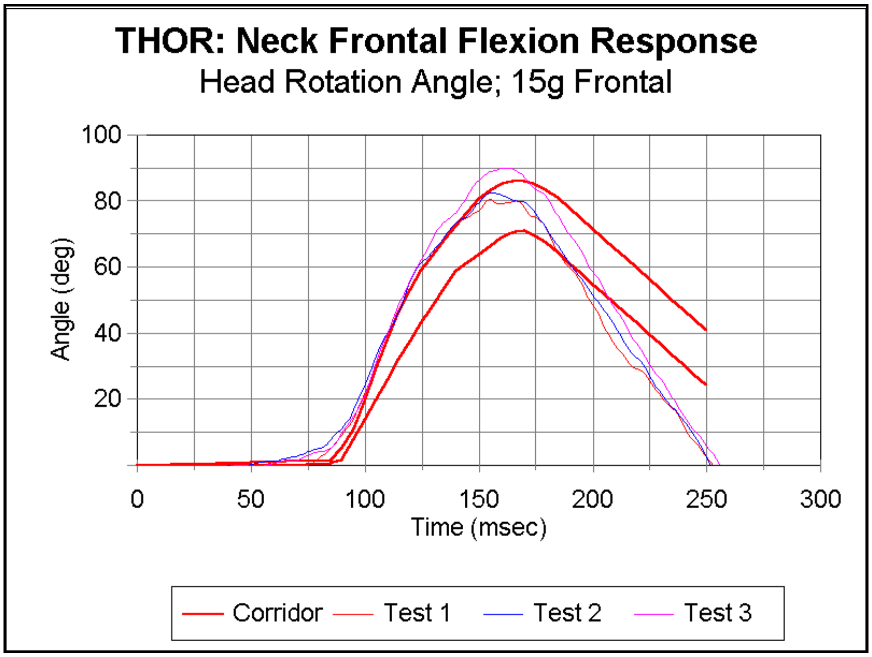


**Figure 36. Head rotation angle time history for neck frontal flexion test.**

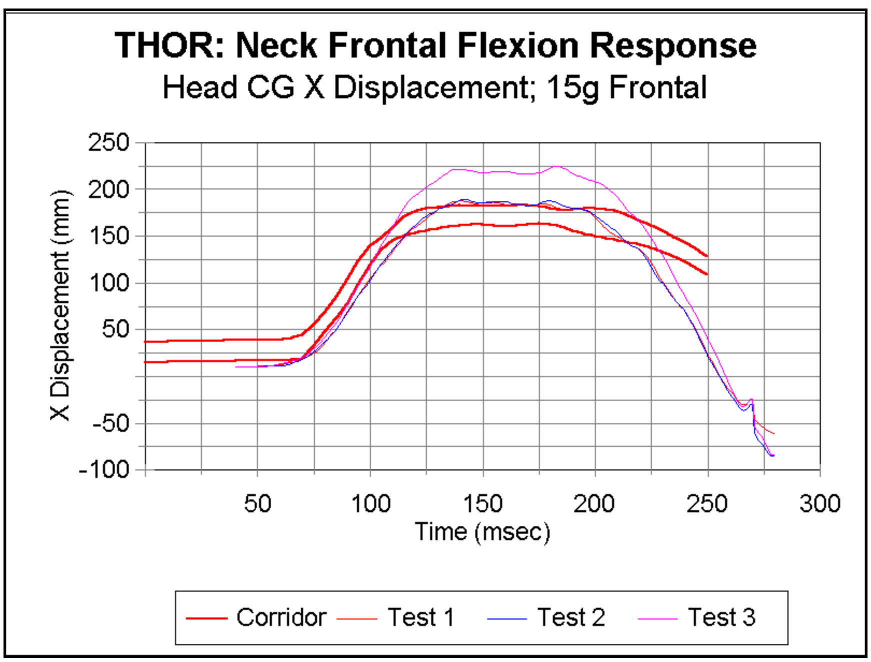


**Figure 37. Head CG X displacement time history for neck frontal flexion test.**

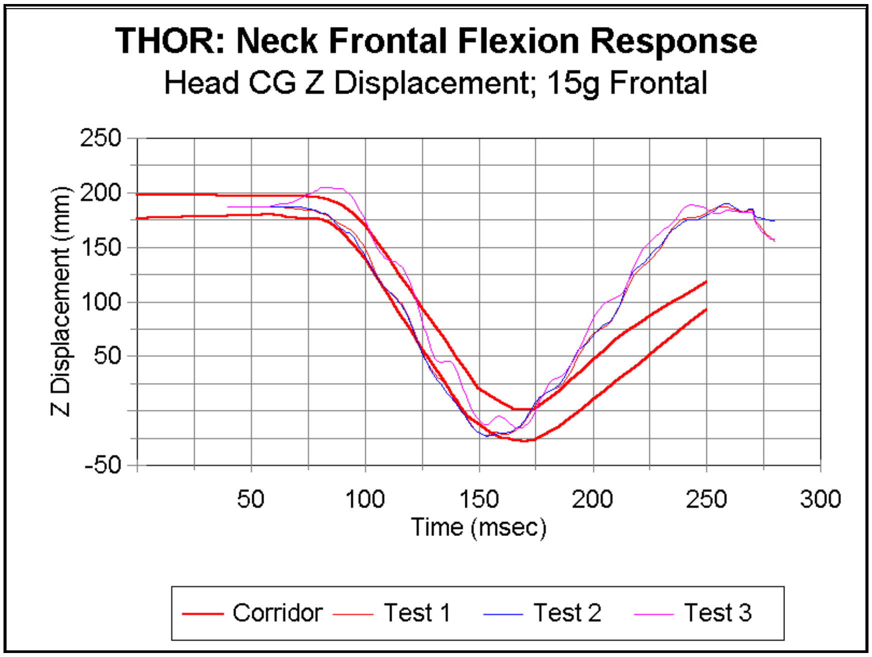


**Figure 38. Head CG Z displacement time history for neck frontal flexion test.**

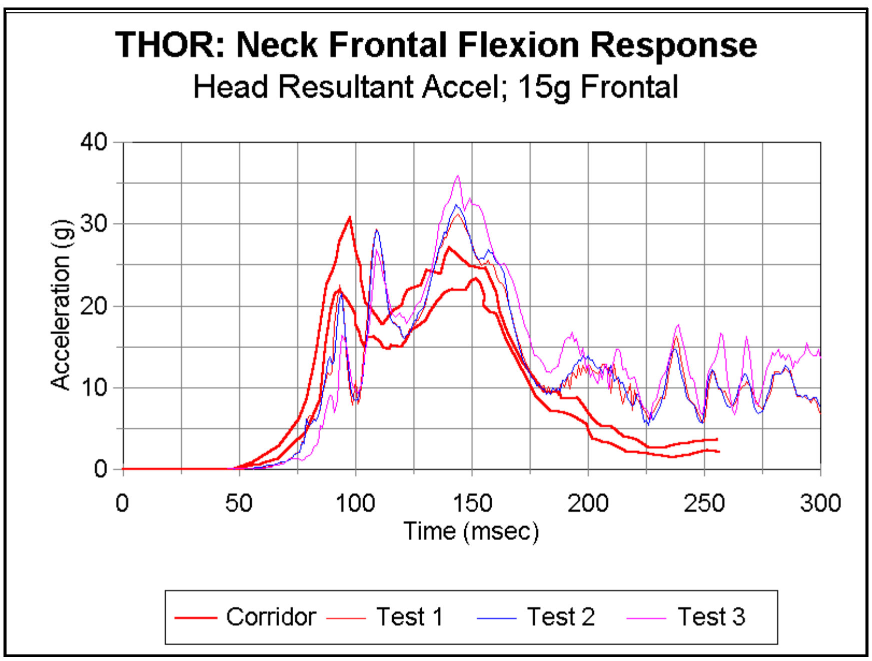


**Figure 39. Head CG resultant acceleration time history for neck frontal flexion.**

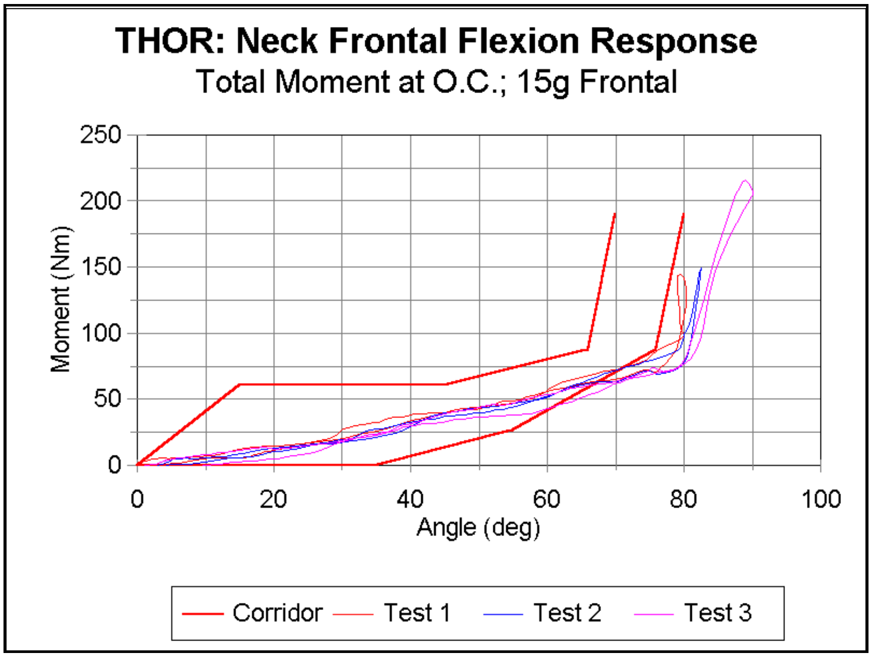

**Figure 40. Moment vs. angle response at O.C. for neck frontal flexion test.**

It is seen that the Thor neck meets the required corridors in frontal flexion though generally at the higher end of the head C.G. displacement corridor. This is also borne out by the moment-angle response seen in Figure 38, where the Thor neck lies just at the bottom of the required corridor.

## 10.2 Lateral Flexion

The following are results obtained from tests conducted at TNO, equivalent to the 7G NBDL lateral flexion tests.

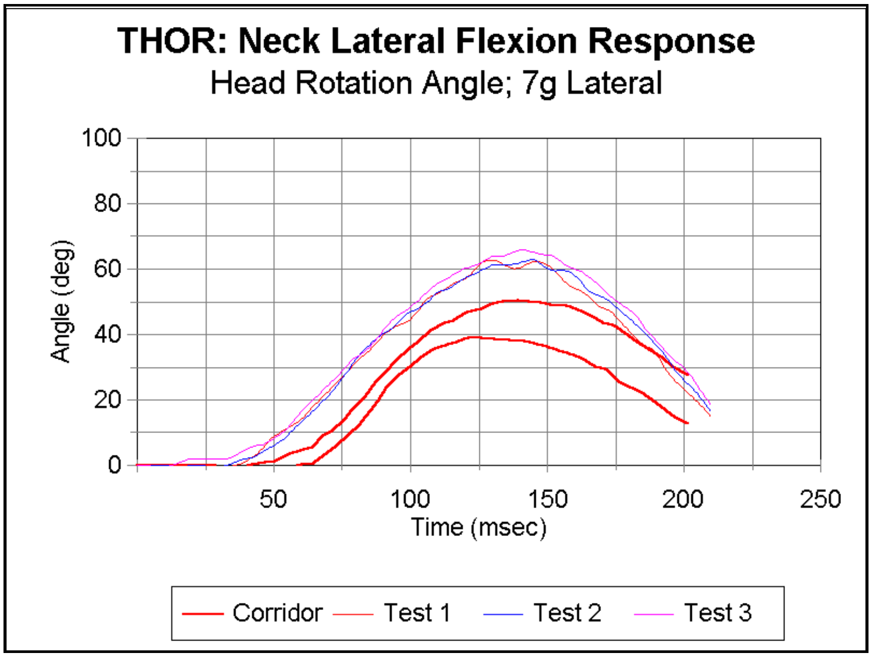


**Figure 41. Head rotation angle time history for lateral flexion test.**

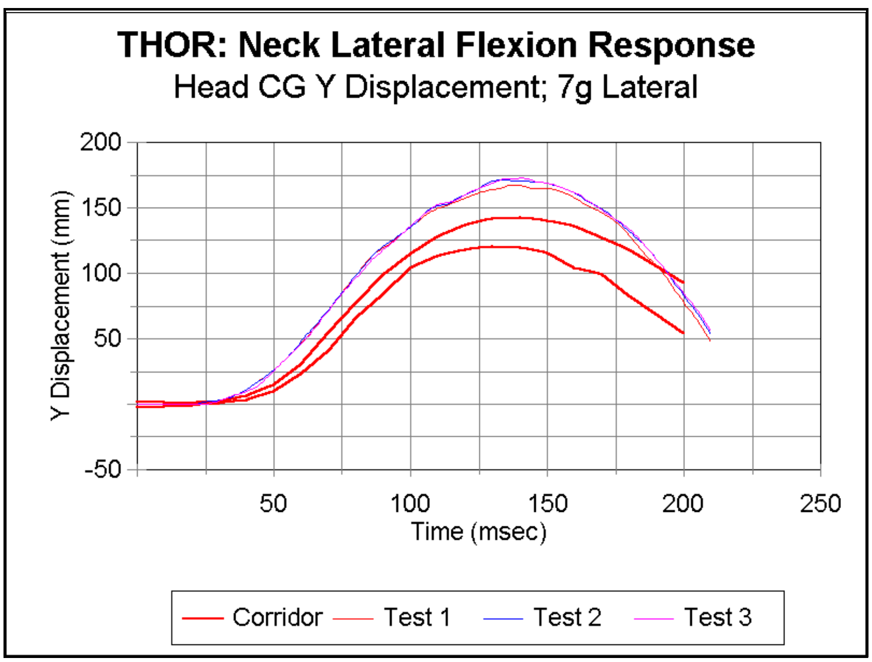


**Figure 42. Head CG Y displacement time history for lateral flexion test.**

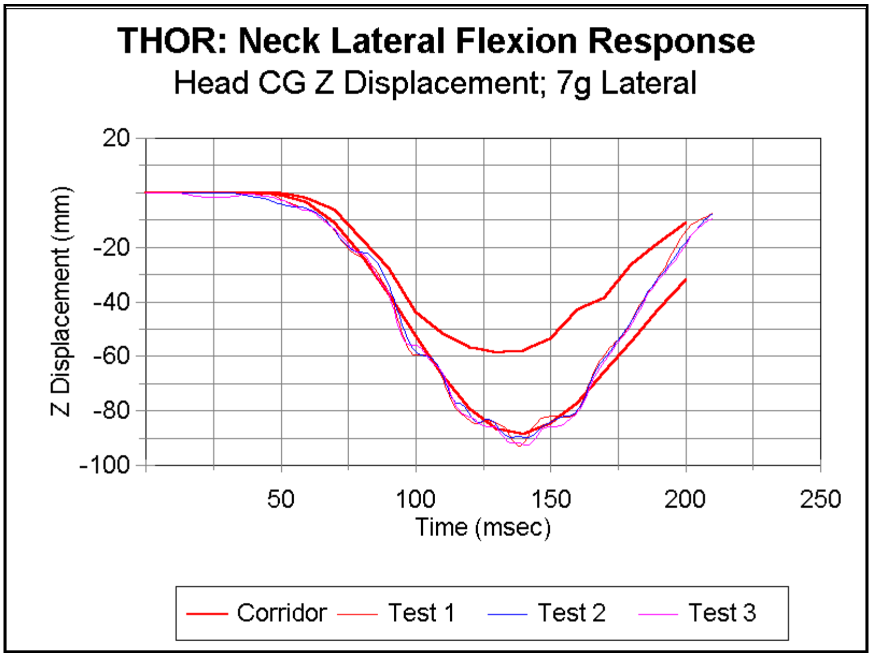


**Figure 43. Head CG Z displacement time history for lateral flexion test.**

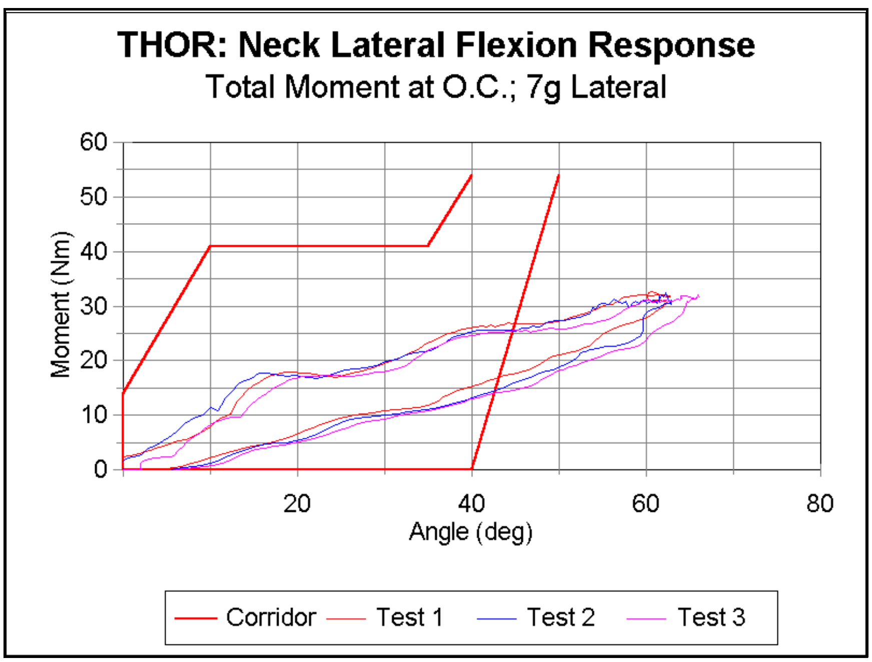


**Figure 44. Moment-angle response at O.C. for lateral flexion test.**

It is seen that the Thor neck lies slightly outside the head angle and the head C.G. Y displacement corridors. The moment-angle response indicates that the neck is within the corridor up to 45°.

## 11. THORAX BIOFIDELITY

### 11.1 Sternal Impact

Extensive series of Kroell-type tests have been performed to evaluate the response of Thor for central, sternal impact. The responses for the 4.3 m/s impact for four different Thor dummies are shown in the following graphs. The deflections of the upper ribcage are measured by the upper Crux measurement system in Thor, and the first graph shows the output from the right side Crux, while the next graph shows the output from the left side Crux.

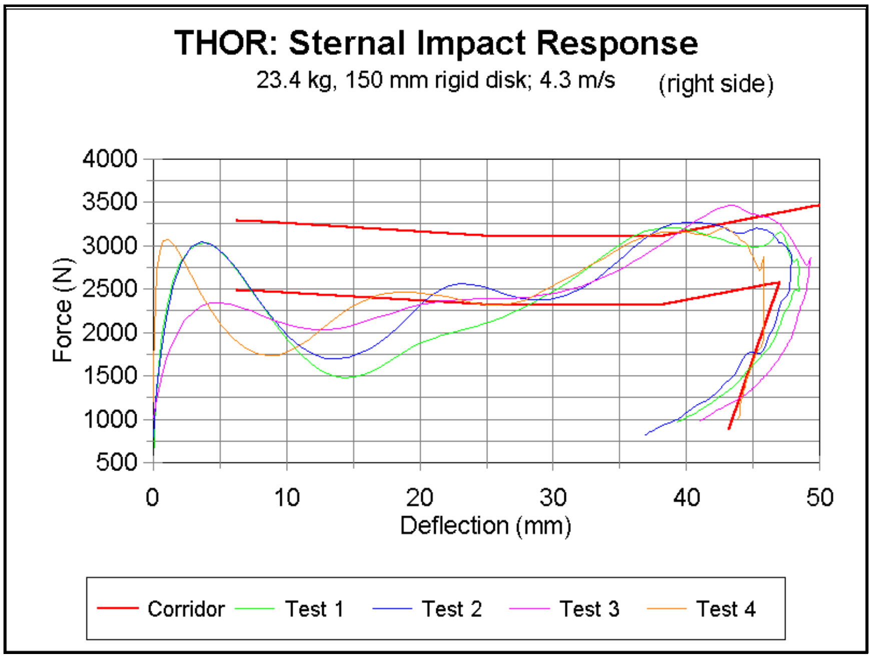


**Figure 45. Response of Thor to sternal impact during Kroell testing at 4.3 m./s impact speed (right side measurements).**

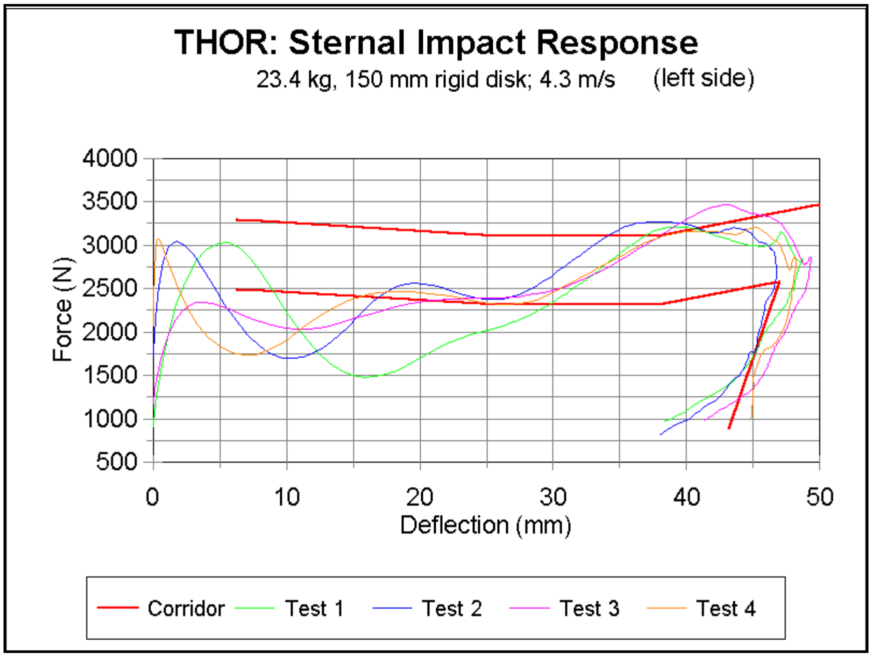


**Figure 46. Response of Thor to sternal impact during Kroell testing at 4.3 m./s impact speed (left side measurements).**

The peak force, maximum deflection, hysteresis, and general shape of the force-deflection curve are reproducible . There is some variation in the peak and timing of the initial force.

The corresponding responses for Kroell tests at impact speed of 6.7 m/s are shown below.

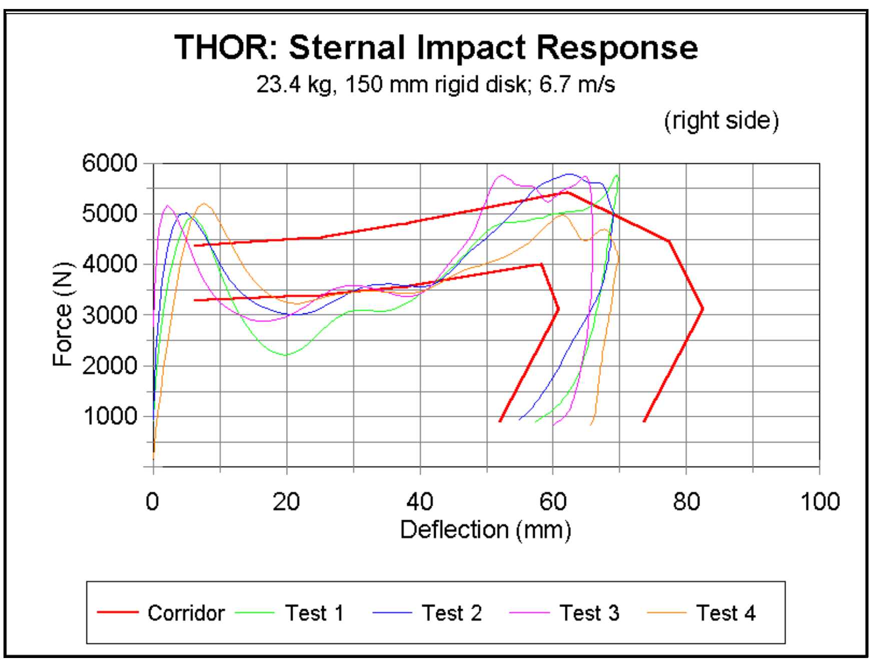


**Figure 47. Response of Thor to sternal impact during Kroell testing at 6.7/s impact speed (right side measurements).**

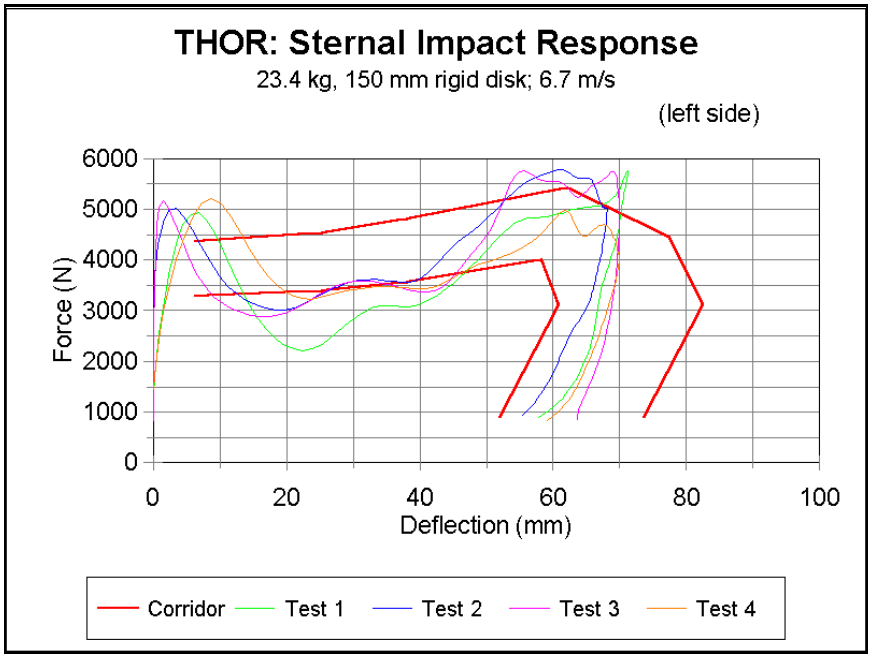


**Figure 48. Response of Thor to sternal impact during Kroell testing at 6.7 m/s impact speed (left side measurements).**

## 11.2 Lower Ribcage Oblique Impact

The response of Thor to oblique impact at the lower ribcage (at impact angle of 15° ), as described in Section 4.2 (MCW test), is shown in the following graph. The penetration is measured using a linear potentiometer attached to the impactor. The external deflection measurement is used in the Thor tests to compare with the external deflection measured on the cadavers using the chestband in the MCW tests. In the normal certification of the Thor lower ribcage only the internal deflection measurement from the Crux will be used.

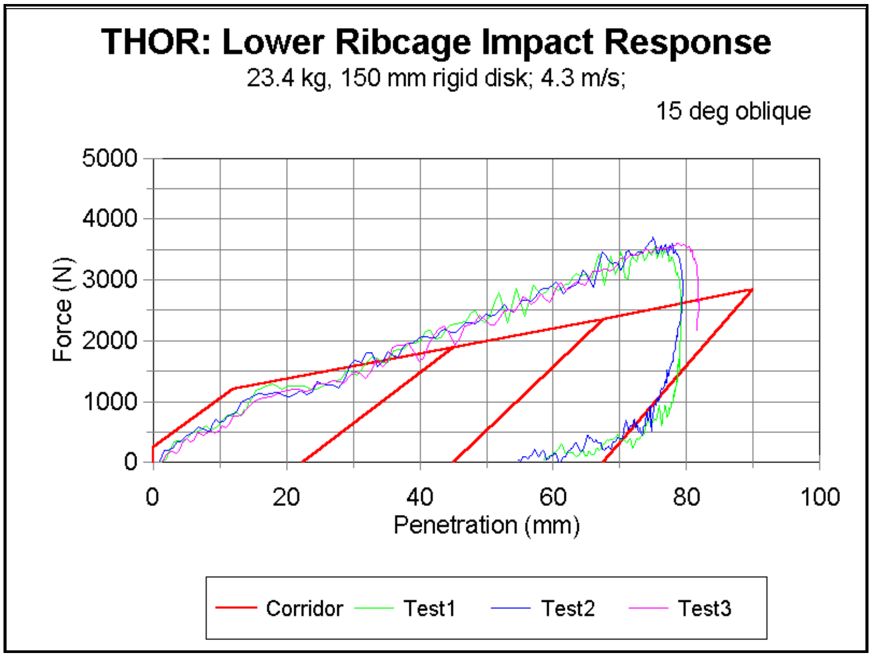


**Figure 49. Response of Thor to lower ribcage oblique impact at 4.3 m./s impact speed.**

The maximum penetration seen in Thor is near the maximum value defined by the corridor. The peak force is higher than seen in the cadaver tests (3500 N in Thor vs. 2800 N for cadavers).

## 12. ABDOMEN BIOFIDELITY

### 12.1 Upper Abdomen: Steering Wheel Impact

The response of Thor to a steering wheel impact to the upper abdomen is shown below.

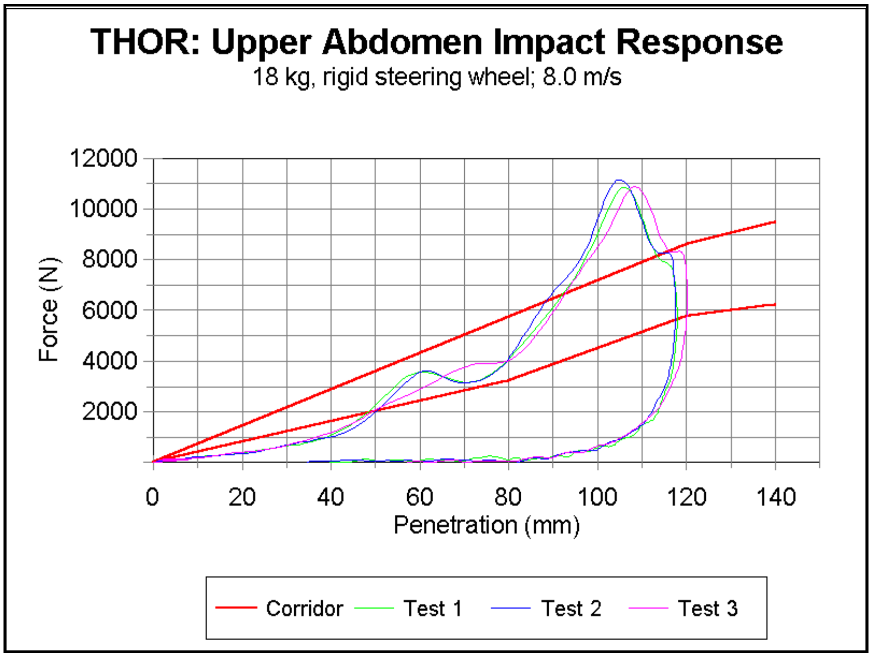


**Figure 50. Response of Thor to steering wheel impact at 8.0 m/s to upper abdomen..**

The repeatability of the response is good and there is general agreement up to 80 - 90 mm of penetration.. Beyond this level of penetration, the impact force increases rapidly, well outside the range seen in the cadaver tests. Thus the dummy is biofidelic for penetrations less than 90 mm..

### 12.2 Lower Abdomen: Rigid Rod Impact

The response of Thor to impact by a 25 cm diameter rigid rod as described in Section 5.2 is shown in the following graph. The penetration is measured by the displacement of the impactor.

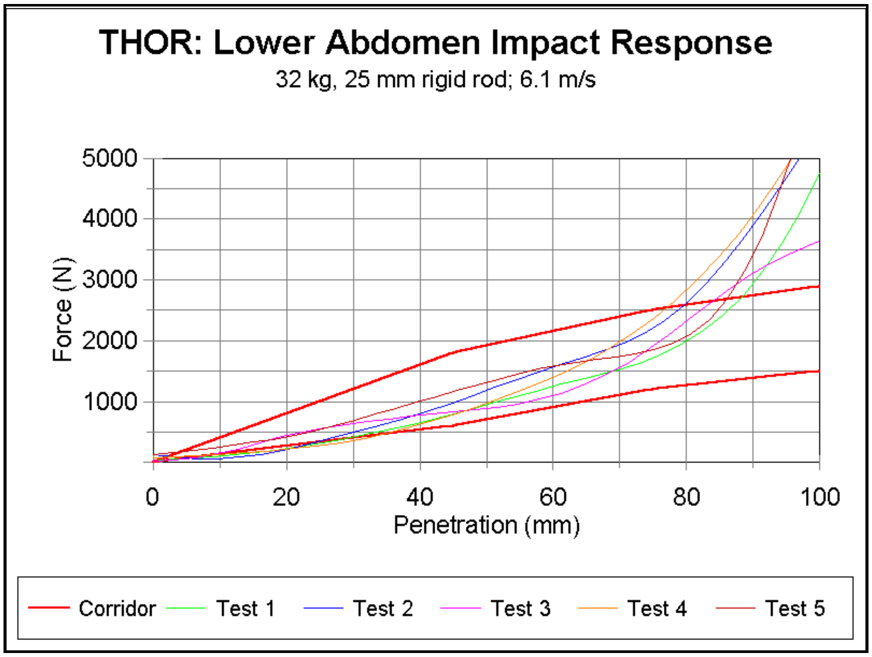


**Figure 51. Response of Thor to rigid rod impact at 6.1 m/s to lower abdomen..**

As in the case of the upper abdomen, the force-deflection characteristics of the Thor abodmen are biofidelic up to 75 - 80 mm of penetration.

## 13. FEMUR BIOFIDELITY

The biofidelity of the Thor knee and femur assembly is determined using the knee impact test of Horsch and Patrick, as described in Section 6. The response is provided as peak impact forces measured for different impact velocities. This is plotted in the graphs below. The plots show the responses from four different Thor dummies, and for both the right and left knees.

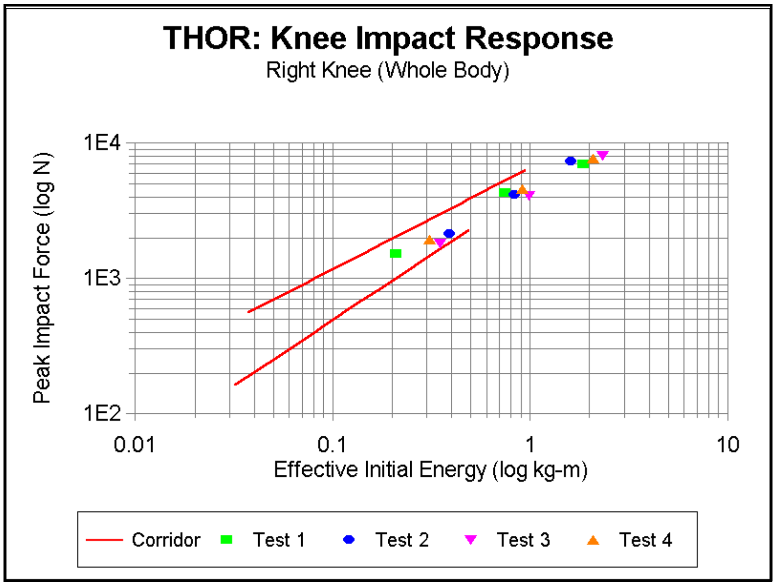


**Figure 52. Response of Thor to axial impacts at the knee at different impact velocities (right knee).**

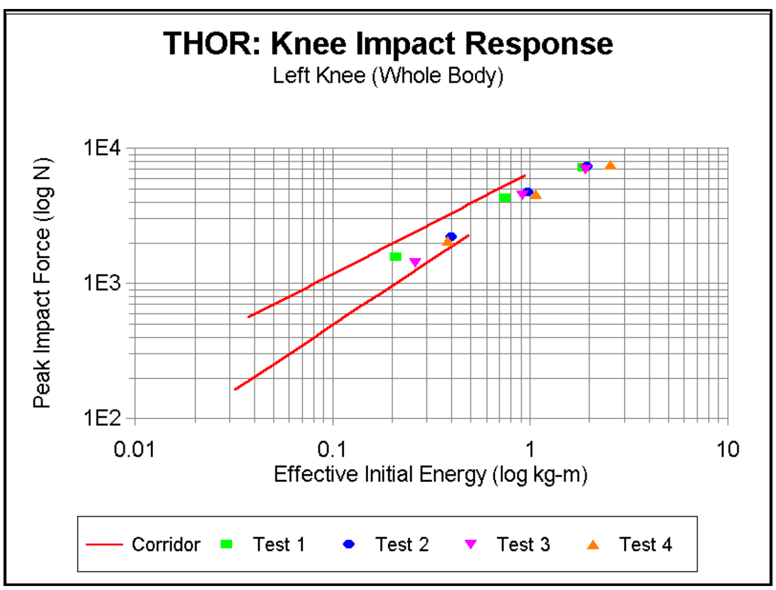


**Figure 53. Response of Thor to axial impact at the knee at different impact velocities (left knee).**

## 14. FACE BIOFIDELITY

There has been limited testing of the Thor face under the test conditions proposed by Melvin, and described in Section 7.1 and 7.2. The response of the face to rod impacts is shown in the following graph.

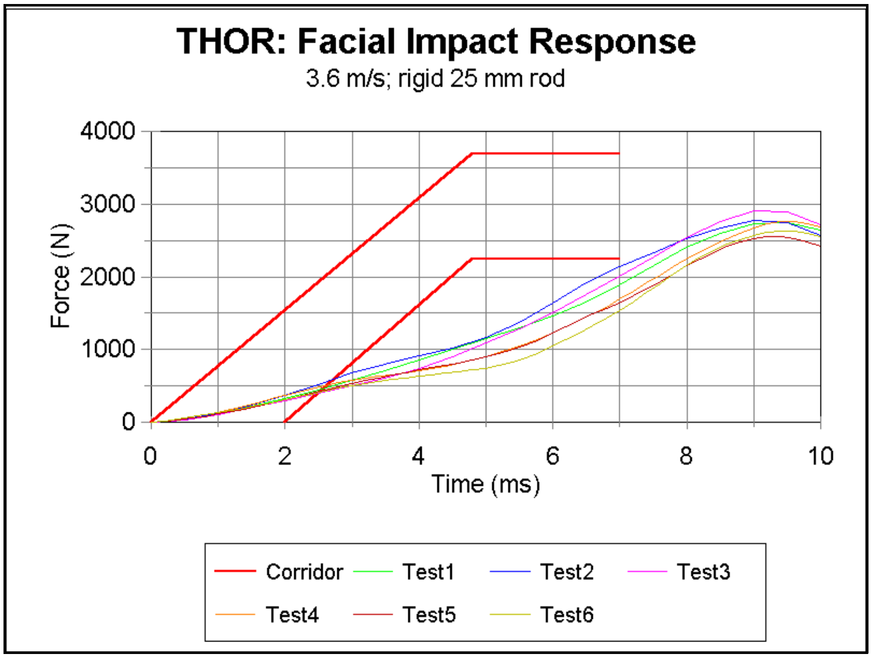


**Figure 54. Response of Thor face to rigid rod impact at 3.6 m/s.**

The responses indicate that the peak forces are well within the human corridors, but that time to reach peak force is delayed by about 2.5 msec.

For the disk impact, the response of the Thor face is shown by the following graph.

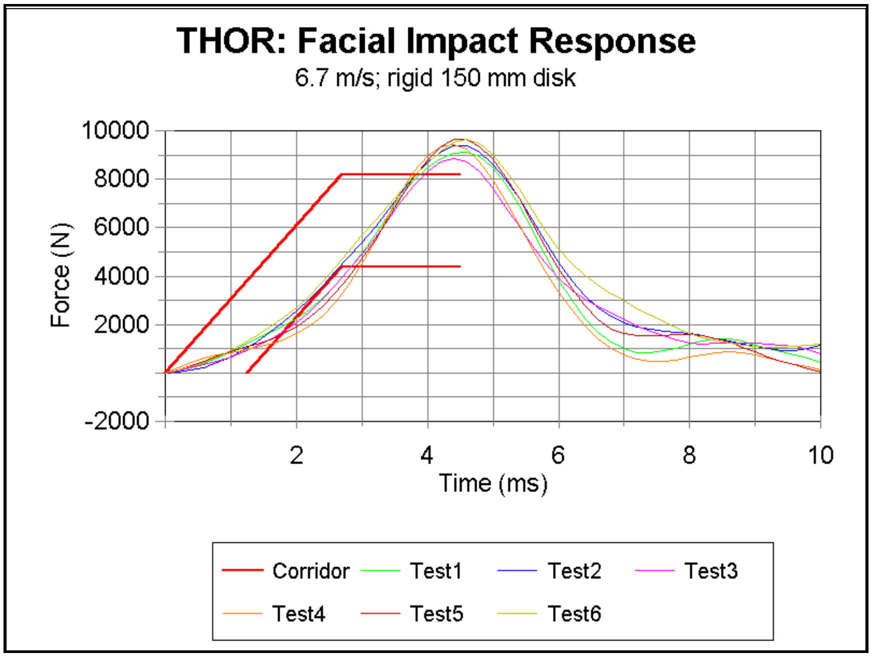

**Figure 55. Response of Thor face to 150 mm disk impact at 6.7 m/s.**

In this case, the peak impact force is some above the corridor, while the timing is within.

## 15. LOWER LEG/ANKLE/FOOT

The biofidelity of the Thor lower leg, ankle, and foot assemblies have been extensively evaluated. The responses are described below.

### 15.1 Dynamic Heel Impact

The response of theThor-Lx (lower extremity of Thor) to an axially directed impact to the heel is shown in the following figure. The test condition is not exactly the same as that described in Section 8.1. In these tests, the proximal end of the tibia was attached to a rigid platform, rather than a mini-sled. Thus the effective moving mass was simply the mass of the impactor.

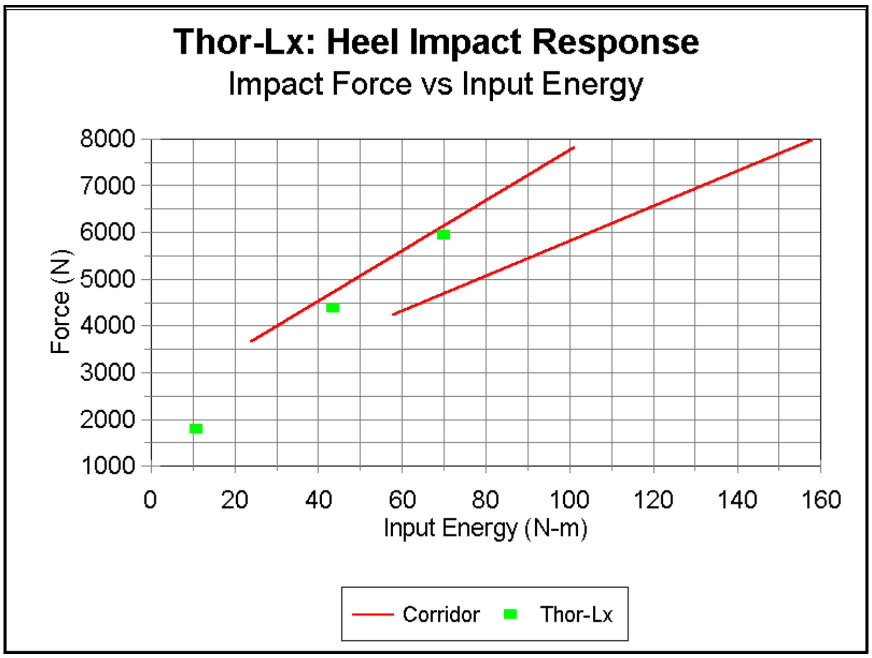


**Figure 56. Response of Thor-Lx to heel impacts at velocities in range of 2.0 m/s to 4.0 m/s (with impactor mass of 8.6 kg).**

UVa performed a series of pendulum impact tests to the plantar surface of the foot, which duplicated the setup used in their cadaver studies. Though, this test was not used as a requirement to establish biofidelity, it was used to verify that the lower leg /ankle /foot assembly was performing properly in an environment where the tibia would be acted on by a dynamic impact force. The following graph shows the comparison of the response of the lower tibia load cell ( Fz) with that measured in a cadaver.

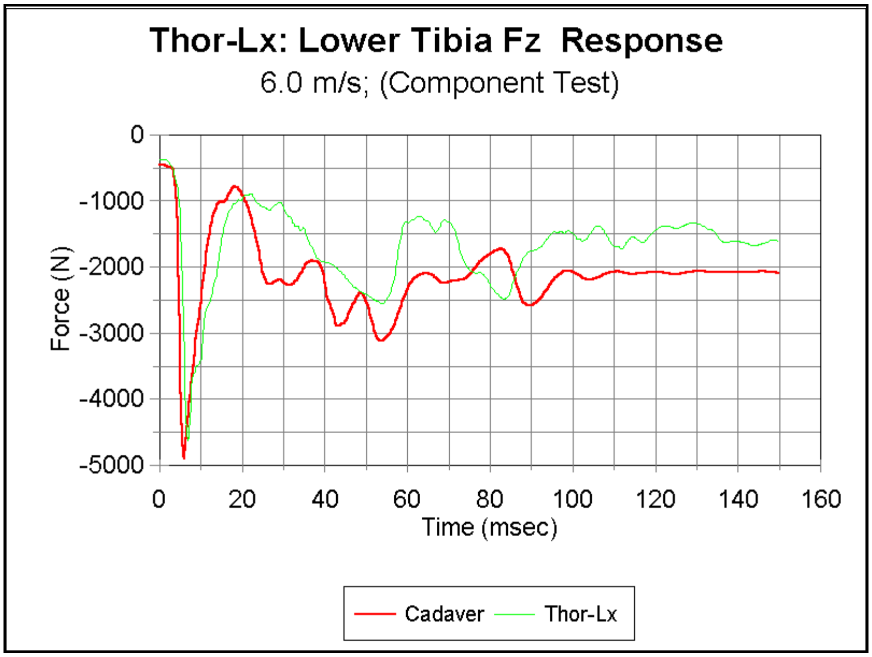


**Figure 57. Comparison of Thor-Lx Fz response in tibia under dynamic axial loading with**

## 15.2 Dynamic Dorsiflexion

The dynamic dorsiflexion response for the Thor-Lx is shown in the following graph. The moments calculated are at the ankle only, since the instrumentation for measuring Achilles tension was not available. The test setup used a simple impact pendulum with a mass of 5 kg, with a cylindrical impact face, which was allowed to impact the ball of the foot.

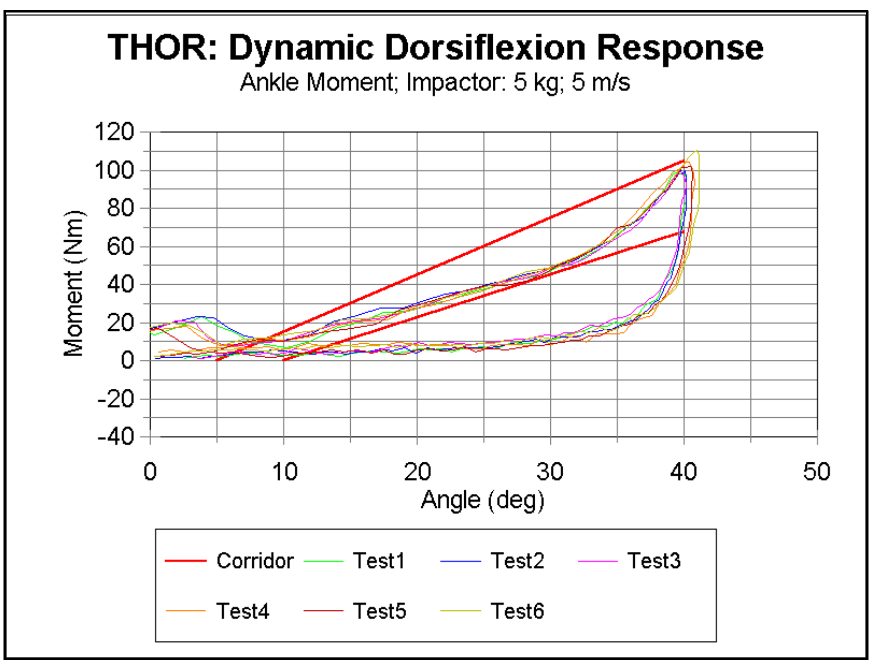


**Figure 58. Moment-angle response in dynamic dorsiflexion.**

## 15.3 Quasi-static Inversion

The response in quasi-static inversion was obtained using a special fixture which is described in the Thor Certification Manual. The fixture allows the rotation of the foot relative to the tibia along each of the ankle axis.

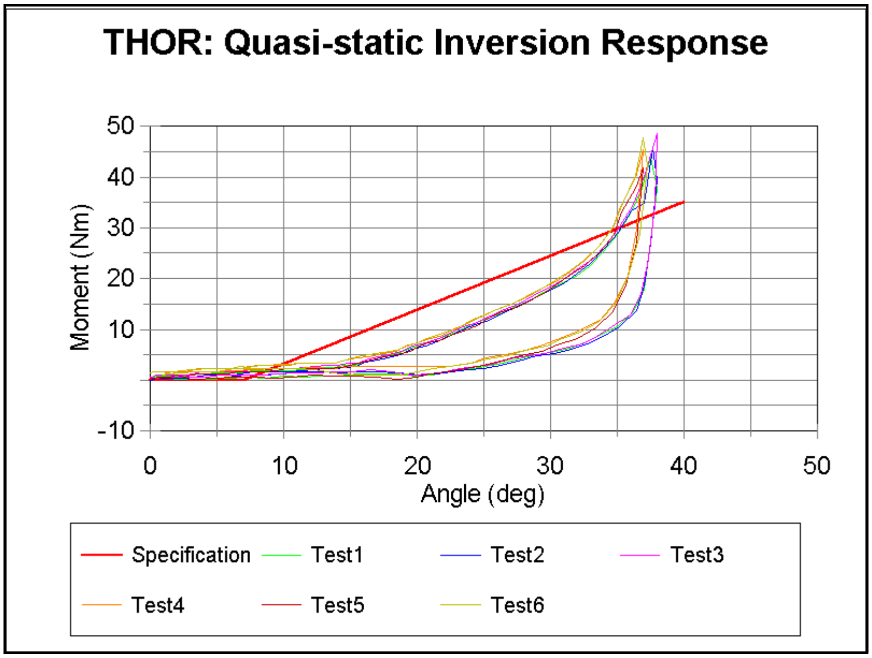


**Figure 59. Moment-angle response in quasi-static inversion.**

## 15.4 Quasi-static Eversion

The response of Thor in quasi-static eversion is shown in the following graph. The fixture used in inversion, is also used here.

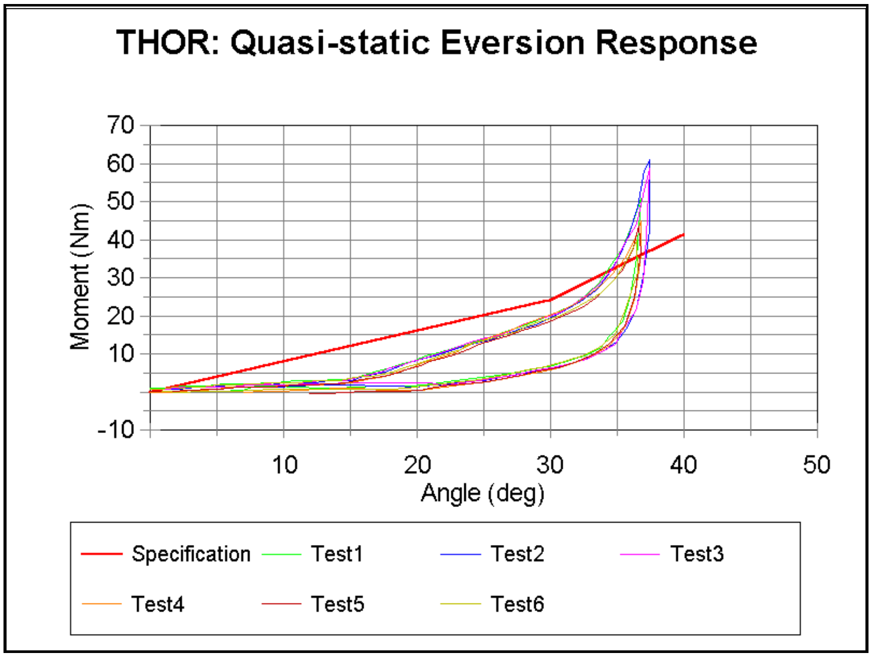


**Figure 60. Moment-angle response in quasi-static eversion.**

### 15.5 Quasi-static Dorsiflexion

Quasi-static dorsiflexion response is shown in the following graph. This response is not a requirement, since the ankle was designed to show appropriate response under dynamic loading as shown in Figure 55. The response shown is for the whole ankle section (i.e. including the influence of the Achilles). It is seen, that under quasi-static loading conditions, the Thor ankle has a stiffer response than human volunteers.

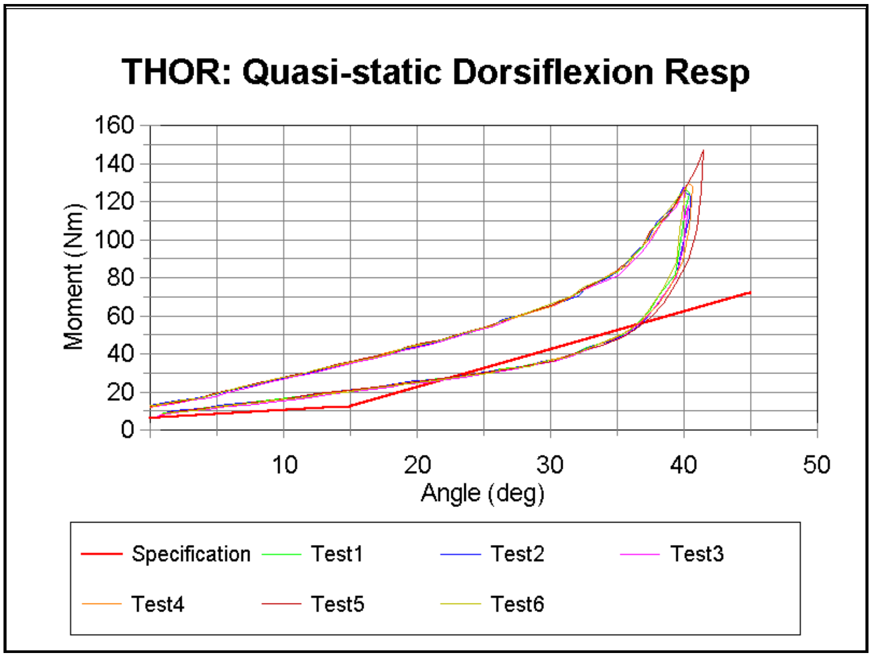


**Figure 61. Moment-angle response at ankle section under quasi-static dorsiflexion.**

## 15.6 Quasi-static Plantarflexion

The response of the Thor ankle under quasi-static plantarflexion is shown in the following graph.

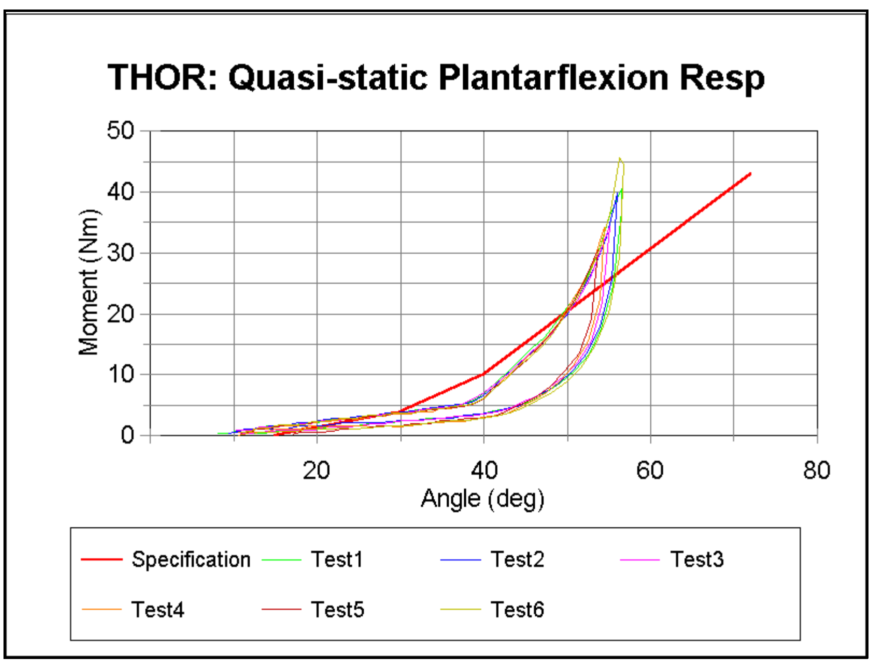


**Figure 62. Moment-angle response of ankle in quasi-static plantarflexion.**

### 15.7 Quasi-static Internal/External Rotation

The response of the Thor ankle assembly in quasi-static internal and external rotations is shown in the following graph.

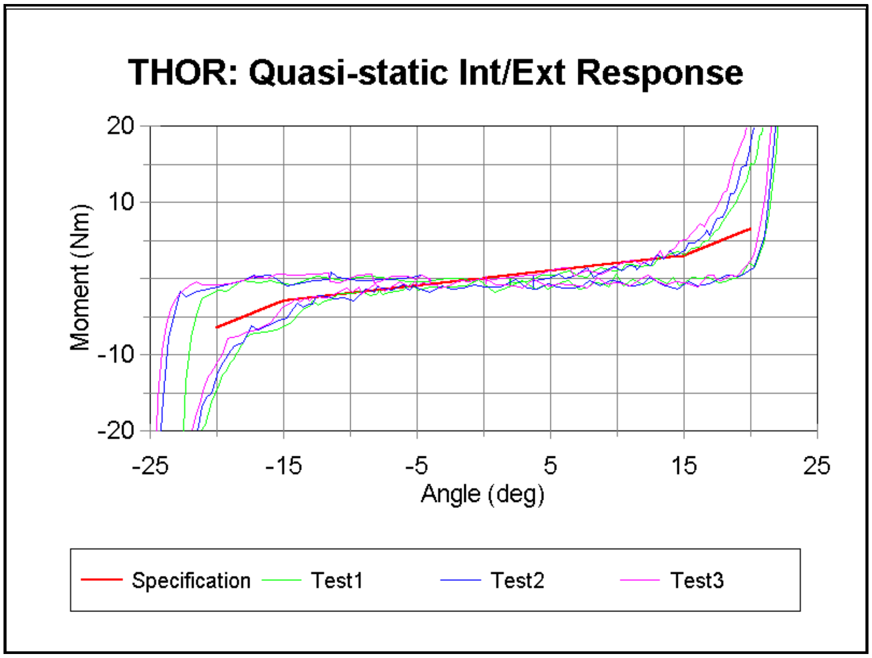


**Figure 63. Moment-angle response in quasi-static internal/external rotation.**

The internal/external joint in the Thor-Lx was designed to provide approximate biofidelity within the range of ±15°. Beyond this point, the ankle is meant to stiffen up in a gradually increasing fashion.

## SECTION III. PROPOSED ADDITIONAL BIOMECHANICAL REQUIREMENTS

## 16. NECK

### 16.1 Neck Kinematic and Dynamic Response in Extension

**References**

Ono, K. et al. 1999. *Relationship between Localized Spine Deformation and Cervical Vertfebral Motions for Low Speed Rear Impacts Using Human Volunteers.* 1999 IRCOBI Conference. pp 149-164.

**Description**

The requirements proposed here are based on the study carried out by Ono et al. [1999]. They studied the response of seven human volunteers under low speed rear-end impact. Subjects were placed on a seat mounted on a small sled system moving on an inclined rail which allowed the seat to slide freely backwards. The system was capable of sliding freely on a 4 meter long rail inclined at an angle of 10°. At the end of travel, it collided with a damper. Tests were conducted at impact speeds of 4, 6, and 8 km/h. A oil shock damper was installed to simulate the accelerations generated during actual real impacts. At the 8 km/h impact, the peak sled acceleration was about 4 G. Both a rigid seat made of wood, and a standard, commercial seat were used. A grip handle was installed in front of the seat to reproduce the extent of each subject's muscular tension.

No headrest was used. The change of the spine configuration was measured by a new spine deformation sensor with 33 paired strain gauges and placed against the spine. The interface load distribution was measured using a Tekscan system running at 100 frame/sec, placed between the seat and the subject. Cineradiography at 90 fps was also used . Measurements included two sets of biaxial accelerations on the head. Markers were placed on the head, neck, and torso to allow for digitization. Motions were measured with high speed camera. The digitized information included: rotation angles of the head, neck, and the upper torso. Spine extension was defined and analyzed as the change in length of the line connecting the neck-torso joint and the iliac crest.

For the biofidelity requirement for Thor, the response at 8 kph impact speed and rigid seat is used as it offers the highest level of severity and the rigid seat ensures reproducibility of the test condition.

**Test Setup**

1. Subject seated on a rigid seat sliding freely on a rail system inclined at 10° without headrest.
2. Impact speed of 8 km/h.
3. Measure accelerations to allow computation of the acceleration of the head C.G. and

angular acceleration of head. Determine motion of markers to allow determination of head angle time history.

For the dummy, a simpler test condition can be defined using only the head-neck system. In this case, the T1 acceleration measured with volunteers, is used as input to the base of the neck.

## Biomechanical Requirement

The acceleration at T1, which could be input to a head/neck assembly is shown in Figure 64. The original sled acceleration is shown in Figure 65. The neck kinematic responses in extension are defined by the Figures 66-69, including head acceleration in the X direction.

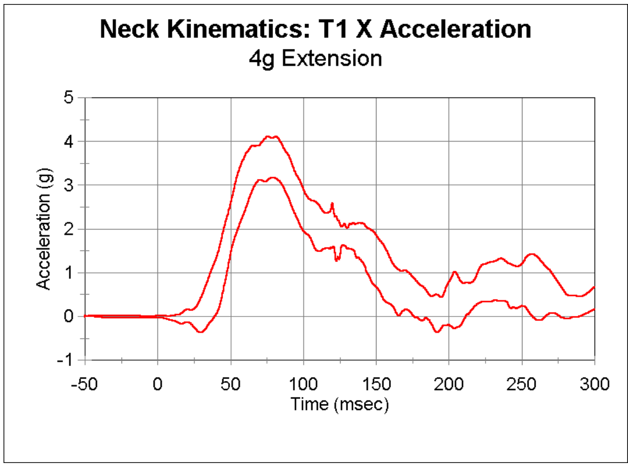


**Figure 64. Corridor for T1 acceleration for extension tests.**

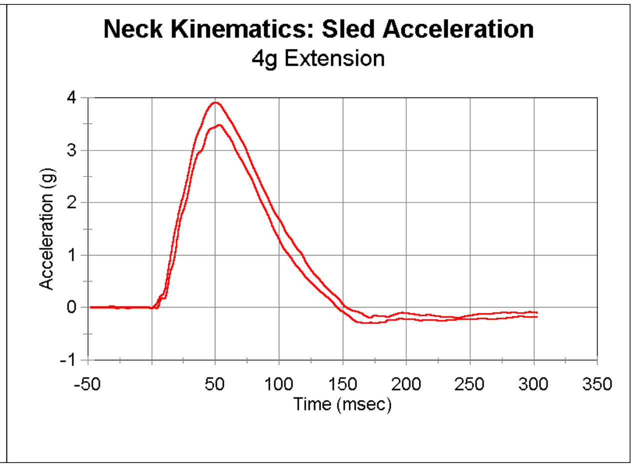


**Figure 65. Corridor for sled acceleration for extension tests.**

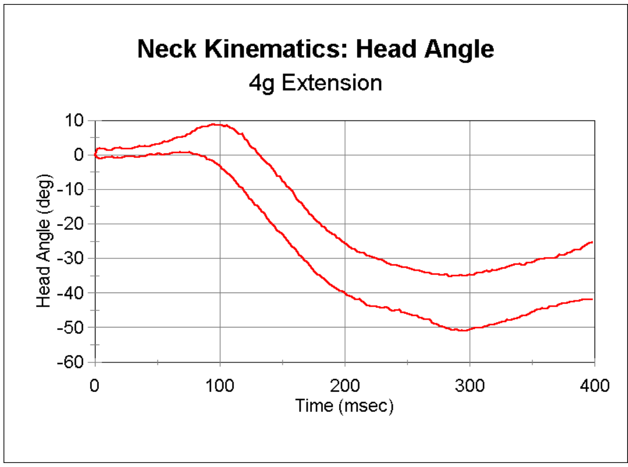


**Figure 66. Corridor of head angle w.r.t T1 for sagittal extension**

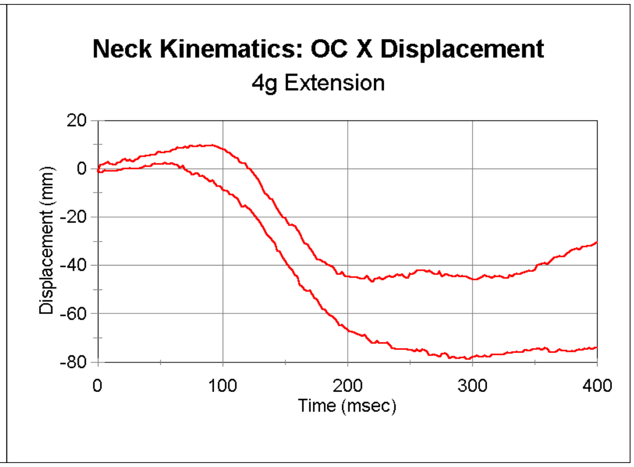


**Figure 67. Corridor for Head CG X displacement w.r.t. T1 for extension.**

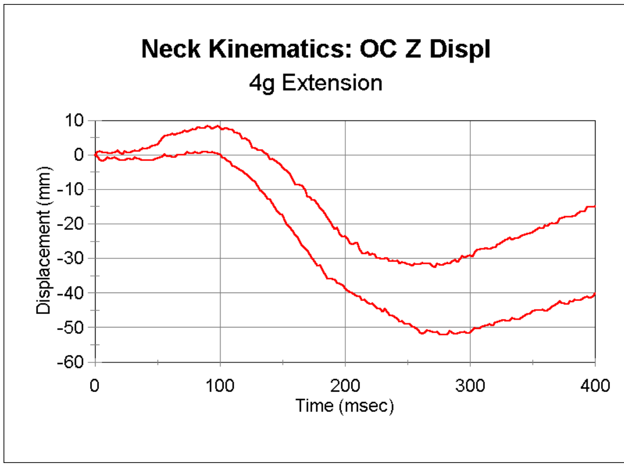


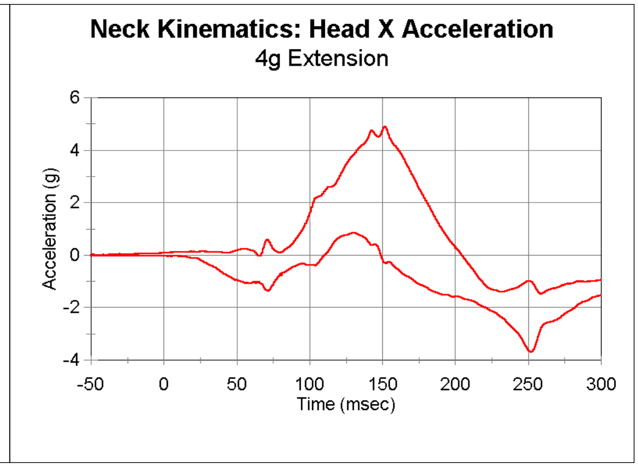


**Figure 68. Corridor for Head CG Z displacement w.r.t T1 for extension**

**Figure 69. Head X acceleration corridor for sagittal extension**

The dynamic response of the neck for sagittal extension is defined by the corridors presented by Mertz and Patrick [1971].

Figure 70 shows the moment-angle corridor of neck during sagittal extension.

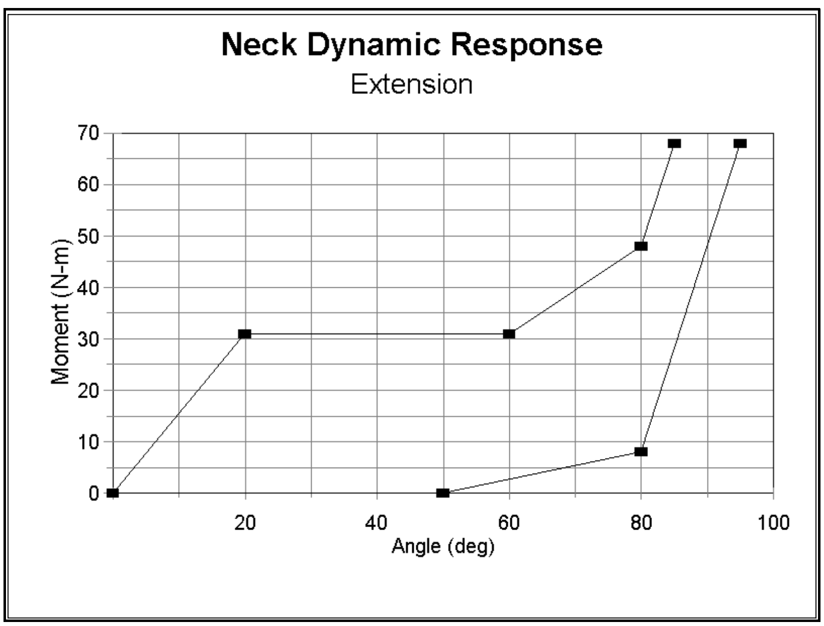


**Figure 70. Moment-angle corridor measured at occipital condyle for extension.**

## 16.2 Neck Axial Compression Dynamic Response

### References

Pintar, F.A., Yoganandan, N., Voo, J., Cusick, J.F., Maiman, D.J. and Sances, A., Jr., 1995. *Dynamic Characteristics of the Human Cervical Spine,* 39th Stapp Car Crash Conference*,* Paper No. 952722.
Pintar, F.A., Sances, A., Jr., Yoganandan, N., Reinartz, J., Mainman, D.J., Suh*,* J.K., Unger*, G.,* Cusick, J.F. and Larson, S.J., 1990. *Biodynamics of the Total Human Cadaveric Cervical Spine,* 34th Stapp Car Crash Conference, Paper No.902309
Nightingale, R.W., McElhaney, J.H., Camacho, D.L., Kleinberger, M., Winkelstein, B.A. and Myers B.S., 1997. *The Dynamic Response of the Cervical Spine: Buckling, Ending Conditions, and Tolerance in Compressive Impacts,* 41st Stapp Car Crash Conference, Paper No. 973344.

### Description

This requirement is used as a secondary requirement for defining the response of the neck. The requirement is based on the study by Pintar et al. [1995]. The tests were performed using a crown impact to the head at speeds ranging from 2.5 m/s to 8 m/s, using 20 unembalmed cadaver head-neck complexes. The failure loads from this study ranged from 744N to 6431N (the mean failure force is 3326N and the standard deviation is 1423N). The deformation at failure was 18 ±3mm. For this test configuration, a force-deformation corridor was derived and given in Figure 70.

Nightingale et al. [1997] also performed a series of neck axial compression tests using unembalmed human head and neck specimens with a drop track system. However, they did not define a corridor for the tests, but gave some numerical guidelines.

### Test Setup

1. The head-neck complex is placed vertically, with the inferior of the neck fixed.
2. The neck is kept straight (pulley and deadweight can be used for this purpose).
3. The diameter of the impactor surface is within 100mm-150mm, and the surface is padded with a 20mm thick ensolite padding.
4. The impact is delivered to the crown of the head.
5. The impactor velocity is between 2.5m/s-8m/s.

### Biomechanical Response

The biomechanical response of neck under axial compression is defined by Figure 70.

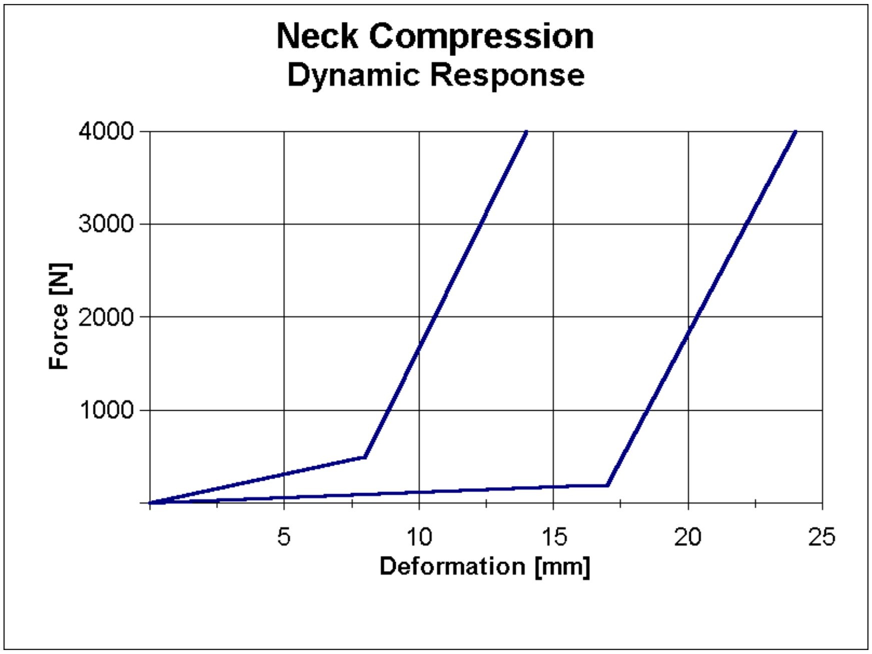


**Figure 71. Force-deformation corridor for neck compression when lordosis is removed [Pintar etc., 1995].**

## 16.3 Neck Tensile Loading Requirement

### References

Van Ee, C.; et al. 2000. *Tensile Properties of the Human Muscular and Ligamentous Cervical Spine.* 44th Stapp Car Crash Journal. Paper 2000-01-SC07.

### Description

This requirement is used as a secondary requirement for defining human neck response. Ee carried out a series of neck tensile tests using six unembalmed cadaver head-neck complexes at a displacement rate of 2mm/s. The effects of the cranial end conditions and load eccentricity were examined. Corridors were given as force-deformation histories. The corridor developed for the fixed end condition has been selected, since this provides the best setup for establishing repeatability in testing.

### Test Setup

1. The head end is fixed so that no motions is allowed.
2. The direction of the loading force is perpendicular to the Frankfurt plane of the head.
3. The displacement rate for the loading is 2mm/s;

**Biomechanical Response**

The force-deflection response to quasi-static loading in tension of a cadaveric head-neck system is given by the graph below.

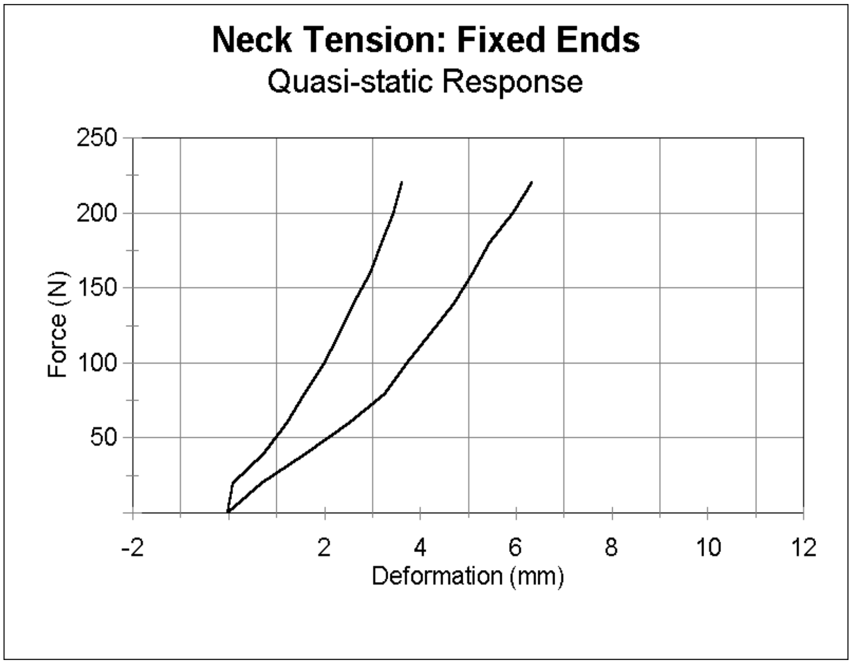


**Figure 72. Force-deformation corridor for neck tensile test under fixed cranial end condition.**

## 16.4 Neck Torsion Requirement

**References**


Myers, B.S., McElhaney, J.H., Doherty, B.J., Paver, J.G., Nightingale, R.W., Ladd, T.P. and Gray, L. 1989. *Responses of the Human Cervical Spine to Torsion*, 33rd Strapp Car Crash Conference, Paper No. 892437.

Wismans, J., and Spenny, C.H. 1983. *Performance Requirements for Mechanical Necks in Lateral Flexion.* Twenty-seventh Stapp Car Crash Conference. SAE Paper # 831613.


**Description**

This requirement is used as a secondary requirement for defining human neck response. The torsion response corridor is based on the study by Myers [1989]. Myers performed a series of neck torsion tests using unembalmed cadaver cervical spines. High velocity failure tests were carried out using ramp-to-failure constant velocity displacements. The lower bound (no muscular action) of the stiffness of the human neck in rotation was derived from these cadaver tests. The upper bound was derived by Myers based on analysis of volunteer sled tests performed by Wismans and Spenny (1983). The target requirement will be based on the dynamic response, since this corresponds to the environment in which the neck will be tested.

### Test Setup

1. The neck assembly is fixed to fixtures at two ends, and is placed horizontally.
2. The axial displacement of the neck should be allowed during the torsion.
3. The test is performed at a high rotational velocity up to 500 degrees/second.

### Biomechanical Response

The torsion response is defined in the graph below.

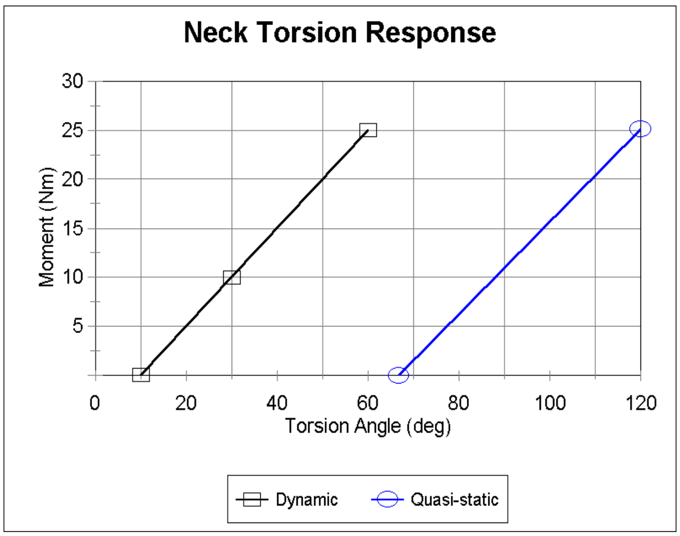


**Figure 73. Response corridor of cervical spine under torsion load**

# 17. SPINE

## References

Cheng, R., Mital, N., Levine, R., and King, A. 1979. *Biodynamics of the living human spine during -Gx impact acceleration.* Proc. 23rd Stapp Car Crash Conference, pp 721-763. SAE, Warrendale, Pa.
Demetropoulos, C.K., Yang, K.H., Grimm, M.J., Khalil, T.B. and King, A.I., 1998, *Mechanical Properties of the Cadaveric and Hybrid III Lumbar Spines*, 42nd Stapp Car Crash Conference, Paper No. 983160.
Demetropoulos, C.K., Yang, K.H., Grimm, M.J., Artham, K.K. and King, A.I., 1998, *High Rate Mechanical Properties of the Hybrid III and Cadaveric Lumbar Spine in Flexion and Extension*, 43rd Stapp Car Crash Conference, Paper No. 99SC18.
Mital, N., Cheng, R., Levine, R., and King, A. 1978. *A new design for a surrogate spine*. Proc. 7th Experimental Safety Vehicle Conference, pp 427-438. U.S. Government Printing Office, Washington, D.C.
Nyquist,, G., and Murton, C.J. 1980. *Static bending response of the human lower torso.* Proc. 19th Stapp Car Crash Conference, pp 513-541. SAE, Warrendale, Pa.
Yogannandan, N., Pintar, F, Sances, A. Jr., Maiman, D. and Myklebust, J., Harris, G. and Ray, G., 1988, *Biomechanical Investigations of the Human Thoracolumbar Spine*, SAE paper No. 881331.

## Description

At the present time, there are limited biomechanical data which properly define the kinematics of the spine under external loading on the whole body. There are test data which measure the response of isolated segments of the spine, but it is difficult to extrapolate this information to how the spine would behave when it is integrated with the complete thorax and pelvis. There are quasi-static data developed by Nyquist and Murton [1975] for the resistance of the whole spinal column from T8 to the pelvis for rotation about the H-point. Dynamic response data were obtained from tests in a NHTSA study [Cheng, etal, 1979; Mital, etal, 1978] which had additional information on the relative motion of the thoracic and lumbar spine segments. From these tests, it was concluded that both segments provided about the same degree of flexibility and that both of these segments had about the same degree of bending stiffness.

There are also quasi-static data on thoracolumbar spine developed by Yoganandan et al. [1988], and quasi-static data on lumbar spine developed by Demetropoulos [1998]. Demetropoulos et al. also performed some dynamic test on human lumbar spines at a displacement rate 4m/s [1999], but the data were too irregular to be considered useful.

## 18. THORAX

### 18.1 Thorax: Regional Coupling under Quasi-static Loading

**Reference**

Schneider, L., et al. 1992. Design and Development of an Advanced ATD Thorax System for Frontal Crash Environments, Volume 1. UMTRI. DOT Report No. DOT HS 808 138

**Description**

A measure of the coupling between different regions of the thorax to localized loading has been developed by Cavanaugh [Schneider, 1992]. He statically loaded the chests of three cadavers using a 5 cm x 10 cm rigid loading plate. Loads were applied at various locations on the sternum and ribcage, and for each loading location, the deflections at eight locations on the anterior thorax were measured. The locations on the sternum were at the upper, mid, and lower sternum. The locations on the ribs were at the 2nd, 5th, and 8th ribs on both the right and left sides.

**Test Setup**

1. Subject was placed in a supine position and loading was applied on the denuded ribcage.
2. The spine and the posterior ribs were supported bilaterally, approximately 7 cm lateral to the midline.
3. Loading rate ranged from 1.3 mm/s to 100 mm/s and stroke set at 2.5 cm.
4. Size of the rectangular loading surface was 5 cm x 10 cm.
5. Loading was applied on the upper, mid, and lower sternum, and at costo-chondral junction of the 2nd, 5th, and 8th ribs. The orientation of the loading surface at the upper and lower ribcage positions resembled the layout of a shoulder belt at these locations.

**Biomechanical Response**

The deflection responses at the eight thorax locations, to the quasi-static loading are shown in the tables below. The expected range of relative deflections are given, with the deflection at the point of loading being specified as 1.0.

**Table 1. Regional deflections to localized thoracic loading**

| **Upper Sternum Load** | | |
|---|---|---|
| Right Ribs | Sternum | Left Ribs |
| 2: 0.6 - 0.8 | U: 1.0 | 2: 0.6 - 0.8 |
| 5: 0.3 - 0.5 | - | 5: 0.3 - 0.5 |
| 8: 0.1 - 0.3 | L: 0.4 - 0.6 | 8: 0.1 - 0.3 |

| Mid Sternum Load | | |
|---|---|---|
| Right Ribs | Sternum | Left Ribs |
| 2: 0.4 - 0.6 | - | 2: 0.4 - 0.6 |
| 5: 0.4 - 0.6 | M: 1.0 | 5: 0.4 - 0.6 |
| 8: 0.3 - 0.5 | - | 8: 0.3 - 0.5 |

| Lower Sternum Load | | |
|---|---|---|
| Right Ribs | Sternum | Left Ribs |
| 2: 0.2 - 0.4 | U: 0.2 - 0.4 | 2: 0.2 - 0.4 |
| 5: 0.5 - 0.7 | - | 5: 0.5 - 0.7 |
| 8: 0.4 - 0.6 | L: 1.0 | 8: 0.4 - 0.6 |

| Right 2nd Rib Load | | |
|---|---|---|
| Right Ribs | Sternum | Left Ribs |
| 2: 1.0 | U: 0.5 - 0.7 | 2: 0.2 - 0.4 |
| 5: 0.2 - 0.4 | - | 5: 0.0 - 0.2 |
| 8: 0.1 - 0.3 | L: 0.2 - 0.4 | 8: 0.0 - 0.2 |

| Right 5th Rib Load | | |
|---|---|---|
| Right Ribs | Sternum | Left Ribs |
| 2: 0.1 - 0.3 | U: 0.1 - 0.3 | 2: 0.0 - 0.2 |
| 5: 1.0 | - | 5: 0.1 - 0.3 |
| 8: 0.5 - 0.7 | L: 0.5 - 0.7 | 8: 0.1 - 0.3 |

| Right 8th Rib Load | | |
|---|---|---|
| Right Ribs | Sternum | Left Ribs |
| 2: 0.0 - 0.2 | U: 0.0 - 0.2 | 2: 0.0 - 0.2 |
| 5: 0.4 - 0.6 | - | 5: 0.1 - 0.3 |
| 8: 1.0 | L: 0.3 - 0.5 | 8: 0.1 - 0.3 |

### 18.2 Thorax: Regional Loading under Belt Impact

**References**

Cesari, D.; Bouquet, R. 1990. *Behaviour of Human Surrogates Thorax Under Belt Loading.* 34th Stapp Car Crash Conference. SAE Paper No. 902310.

**Description**

Cesari and Bouquet [1990] performed a series of belt impact tests on cadavers to examine the deflections at different points on the chest under belt loading. A belt with a layout resembling a shoulder belt was pulled dynamically against the thorax and deflection measurements were made at 11 locations, which included points on the sternum, upper and lower ribcages. Locations both adjacent to the belt and relatively further away were monitored. The belt was connected to a cable and pulley system which could be activated using an impactor.

**Test Setup**

1. Subjects were supine on a rigid, flat table with belt strap placed diagonally across the chest between the shoulder and the lower ribcage.
2. The two ends of the belt were connected to a cable and pulley system which could be hit by an impactor.
3. Two impactor masses (22.4 kg and 76.1 kg) were used. The impact speeds with the lighter impactor ranged from 2.8 to 9.3 m/s, while impact speeds with the heavier impactor ranged from 2.5 to 3.5 m/s.
4. Vertical deflections of the ribcage (inside flesh) were taken at the clavicle (opposite belt), upper sternum, lower sternum, anterior portion of the fifth and seventh ribs. Horizontal deflections were measured on the lateral portion of the eighth rib. Vertical deflection measurements were also taken along the belt path at the left clavicle, mid sternum, and lower ribcage (around the seventh rib).

**Biomechanical Response**

Preliminary response defined by the belt loading test is relative deflections at different points of the thorax. This is given the following table.

**Table 2. Regional relative deflections to dynamic belt loading**

| Right side | Sternum | Left side |
|---|---|---|
| Clavicle: 0.3 - 0.5 | Upper: 0.5 - 0.9 | Clavicle: 0.5 - 0.9 |
| Rib 5: 0.8 - 1.2 | Mid: 1.0 | Rib 5: 0.1 - 0.3 |
| Rib 7: 1.0 - 1.4 | Lower: 0.8 - 1.1 | Rib 7: 0.1 - 0.3 |
| Rib 8 (y): -0.3 - -0.5 | | - |

# 19. ABDOMEN

## 19.1 Abdomen: Belt Impact

### Reference

Hardy, W.; Schneider, L. 2001. *Development and Refinement of Abdominal-Response Corridors.* UMTRI Report UMTRI-2000-10.

Rouhana, S.W., Viano, D.C., Jedrzejczak, E.A., and McCleary, J.D., 1989. *Assessing Submarining and Abdominal Injury Risk in the Hybrid III Family of Dummies*. 33rd Stapp Car Crash Conference, Paper No.892440.

### Description

Hardy and Schneider [2001] have recently developed a corridor for force vs. penetration of a belt into the abdomen at the level of the umbilicus. Tests were conducted using three cadavers with repeat tests on each. This corridor is different from that developed by Rouhana [1989], who had scaled the data from porcine tests. In the new tests, the belt essentially circled half the abdomen while in the previous tests the belt was straight and was only in tangential contact at the beginning of the load sequence. It is felt that the new configuration is closer to the setup seen by an occupant in a vehicle.

### Test Setup

1. Subjects were placed in a seated, upright position with legs positioned forward and the hands placed in front of and above the head. The subject was placed on a curved,Teflon skid.
2. A standard seat belt (6% stretch) was placed about the mid-abdominal region, approximately at the level of the umbilicus. The webbing was in contact with the anterior aspect of the abdomen and routed around the sides so that the two ends were tangent to the lateral aspect of the abdomen.
3. The belt was loaded on to the abdomen with a peak loading rate of about 3 m/s with the loading pulse having the shape of a half sine wave.
4. Measurements were made of the loads at the two ends of the seat belt and the penetration into the abdomen.

### Biomechanical Response

The response to belt loading about the mid abdomen is given by the following

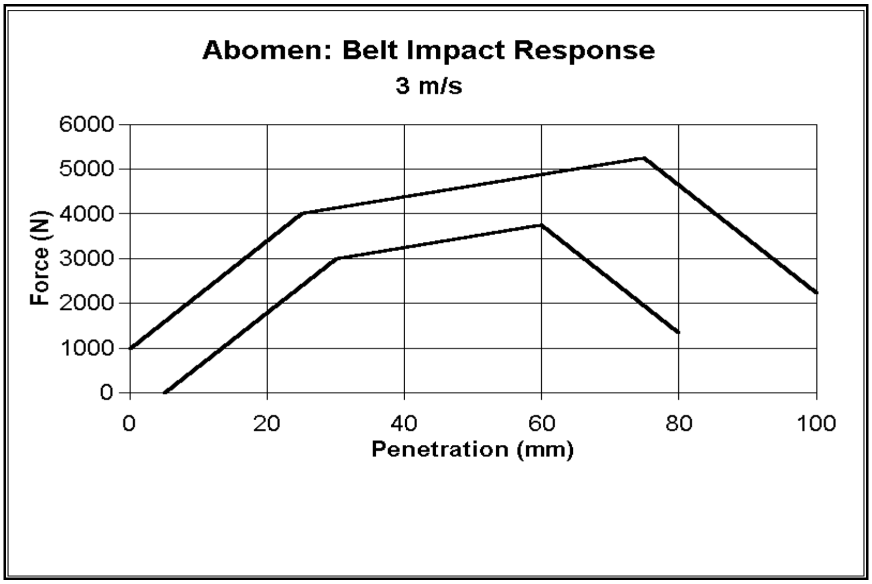


**Figure 74. Corridors for belt impact response with mid abdomen at 3 m/s.**

## 19.2 Abdomen: Airbag Impact

### Reference

Hardy, W.; Schneider, L. 2001. *Development and Refinement of Abdominal-Response Corridors.* UMTRI Report UMTRI-2000-10.

### Description

Hardy and Schneider [2001] have recently developed a corridor for force vs. penetration of an airbag against the abdomen. They developed a surrogate device for the airbag, which was a thin-walled, aluminum cylinder with the cylindrical face impacting the abdomen. The ends of the cylinder were capped with rounded faces to eliminate sharp loads as the cylinder penetrated the abdomen. The fixture is meant to simulate the early stage of a deploying airbag. The device was driven by a pneumatic cylinder and excess pressure is allowed to be vented to the atmosphere. The impact speed was set at about 13 m/s. The final corridor was based on the results from tests on three cadavers.

### Test Setup

1. Subjects were placed in a seated, upright position with legs positioned in front of the cadaver, and the hands placed in front and above the head. The backs of the subjects were supported.
2. The center of the surrogate airbag device was aligned with the umbilicus at the level of the L3 verterbra.
3. The impactor face was the cylindrical side of 7.6 cm diameter tube of length 20 cm, and mass 1 kg. The impactor face was initially placed in front of the abdominal surface.

4. Impact speed was set at 13 m/s.
5. Measurement of the impact load due to the surrogate device surface was made using the acceleration of the device and the internal pressure within the cylinder.

## Biomechanical Response

The response to airbag impact to the mid abdomen is given by the following.

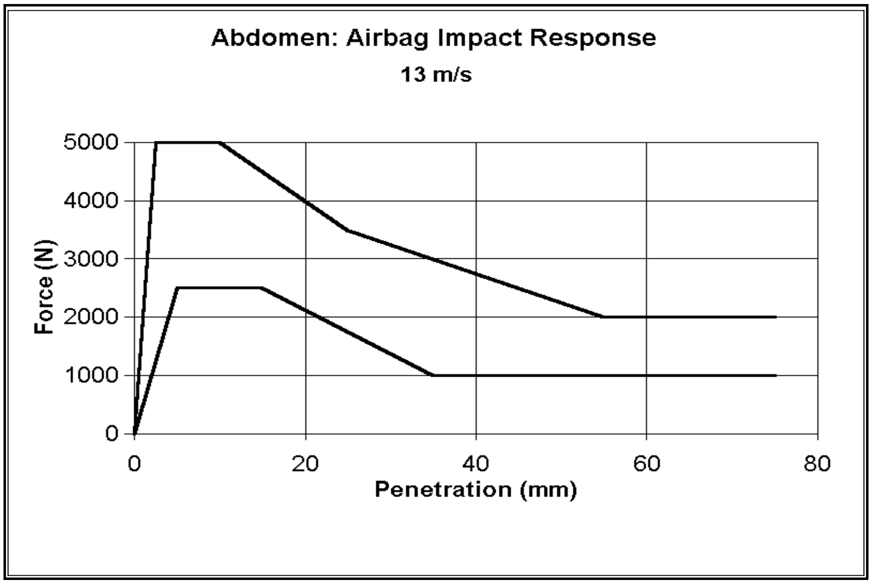


**Figure 75. Force-penetration corridors for airbag impact with abdomen at 13 m/s.**

# 20. FACE

## 20.1 Cylindrical Impactor Response

### References

Bermond, F., Kallieris, D., Mattern, R., Ramet, M., Bouquet, R., Caire, Y. and Voiglio, É., 1999, *Human Face Response at an Angle to the Fore-aft Vertical Plane Impact*, IRCOBI Conference 1999, pp.121-132.

### Description

The corridors here are based on the test data by INRETS [Bermond, 1999]. A total of 57 facial impact tests were performed using a cylindrical impactor simulating a steering wheel rim. The impacts were delivered to the forehead, zygoma and maxilla at an angle of 30 degrees to the fore-aft vertical (sagittal) plane in order to represent typical accidents conditions. The corridors here are impactor peak force and resultant acceleration at head C.G. vs impact velocity for three different regions of the face.

### Test Setup

The test configuration of this test is defined as:

1. The impactor is guided, the mass of the impactor is 17.0kg.
2. A 2.25 cm diameter steel cylinder is mounted horizontally at the far extremity of the impactor and hits the face directly.
3. The impact speed is at 3m/s.
4. The impact should be delivered at an angle of 30 degrees with regard to the fore-aft vertical plane.

### Biomechanical Response

The corridors for forehead, zygoma and maxilla are shown in Figures 75 - 80.

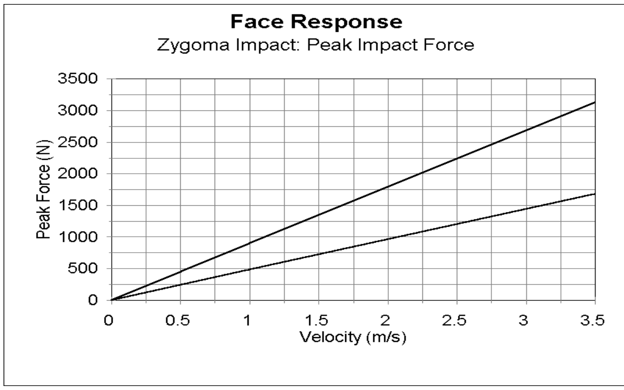


**Figure 76. Corridor for impactor peak force when hitting zygoma**

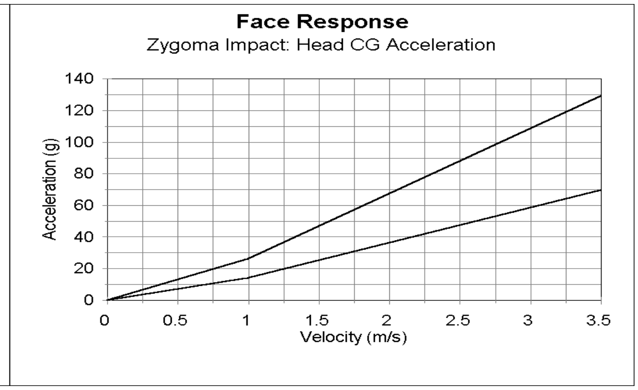


**Figure 77. Corridor for resultant peak acceleration at head CG when hitting zygoma**

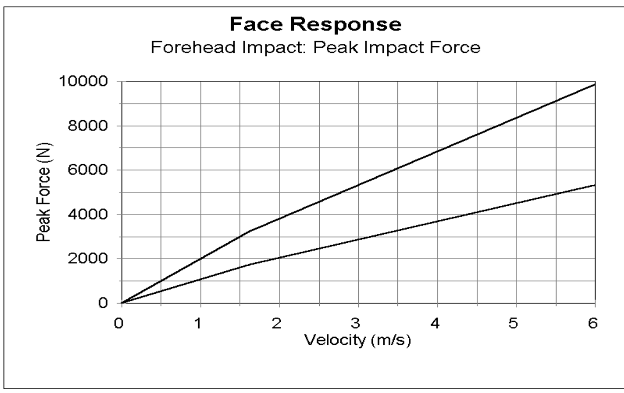


**Figure 78. Corridor for impactor peak force when hitting forehead**

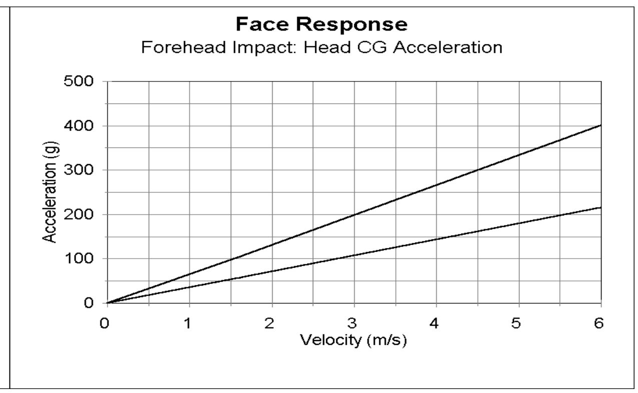


**Figure 79. Corridor for resultant peak acceleration at head CG when hitting forehead**

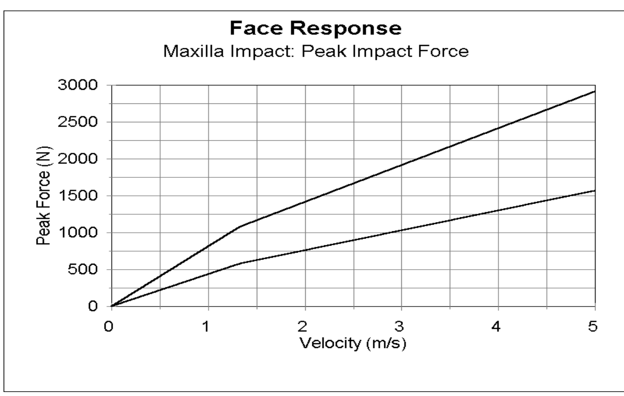


**Figure 80. Corridor for impact peak force when hitting maxilla**

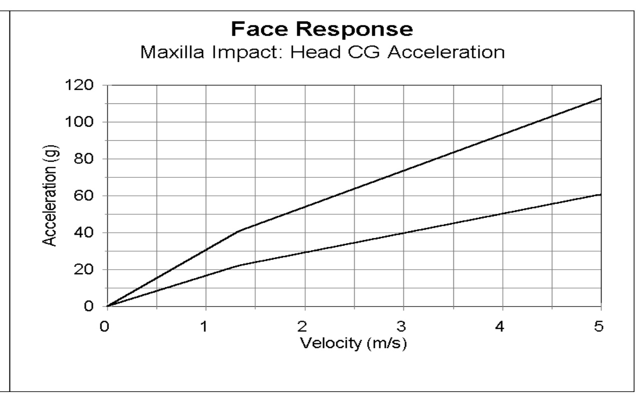


**Figure 81. Corridor for resultant peak acceleration at head CG when hitting maxilla**

# 21. LOWER LEG/ANKLE/FOOT

## 21.1 Dynamic Inversion/Eversion

### References

Jaffredo, A., et al. 2000. *Cadaver Lower Limb Dynamic Response in Inversion-Eversion.* 2000 International IRCOBI Conference on the Biomechanics of Impact. pp 183-194.

### Description

Jaffredo, et al. [2000] studied the dynamic response of the ankle in inversion-eversion. Six pairs of cadaver lower limbs were tested with six tests in inversion and six tests in eversion. Accelerations, angular velocities, forces, and moments were measured on the forefoot, heel, and leg. Force balance was computed at the subtalar joint. The contribution of the fibula was also measured and the angle between the forefoot and heel computed. The subtalar joint moment was evaluated with respect to the xversion angle of the forefoot and of the heel.

In these tests, the lower extremity was amputated at the knee an mounted to the test apparatus. All musculature was preserved. In half the tests, only the forefoot was fixed to the plate, and in the other half, both the forefoot and heel were fixed.. The fixation points corresponded with the anatomic support points of the foot defined by previous X-rays.

Load cells were planted within the tibia and the fibula to determine their contributions to the total axial and shear forces and to the X-axis moment. They also found that the fibula could contribute up to 17.5% of the total moment in the subtalar joint and 50% of the total axial force. This indicated that the fibula can play a significant role in the overall response of the ankle. In several previous studies, the contribution of the fibula was ignored, since only the tibia load cell was inserted. They also estimated the axial force due to passive muscle in inversion and eversion. It was linear as a function of xversion angle. A resistive force of 150 N was generated for a calcaneal angle of 15°. Unlike dorsiflexion, the passive musculature had no significant contribution to the xversion moment.

### Test Setup

1. Lower extremity amputated at knee. Proximal end fixed to a slider, while foot fixed to a rigid, rotating plate, which allows foot to be moved in inversion/eversion.
2. Foot positioned so plate rotation axis is superimposed on the xversion axis defined from X-rays.
3. Foot set at about 90 deg relative to tibia.
4. Impact ball of foot at 2 m/s.
5. Measure forces and moments at distal tibia and fibula, and angle of rotation of calcaneous about center of xversion. Compute moment-angle response at the subtalar joint.

## Biomechanical Response

The moment-angle response corridors for dynamic inversion and eversion, estimated from the cadaver tests are shown in the following graphs. The angle is the measured angle of the calcaneous relative to the tibia. Comparison with the previous quasi-static response curves are shown.

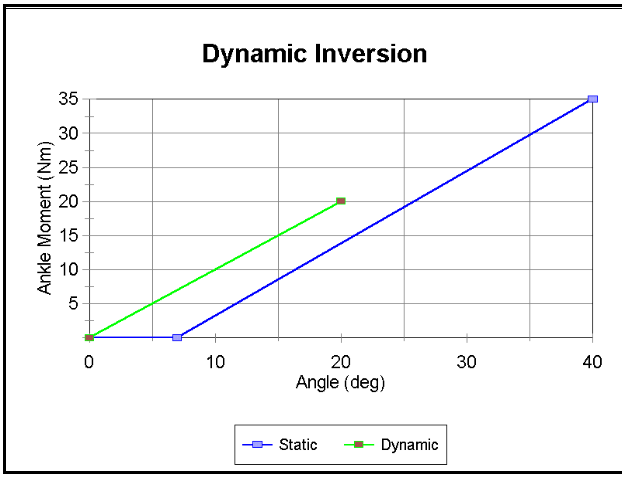


Figure 82. Moment vs angle response for dynamic inversion (and comparison to static).

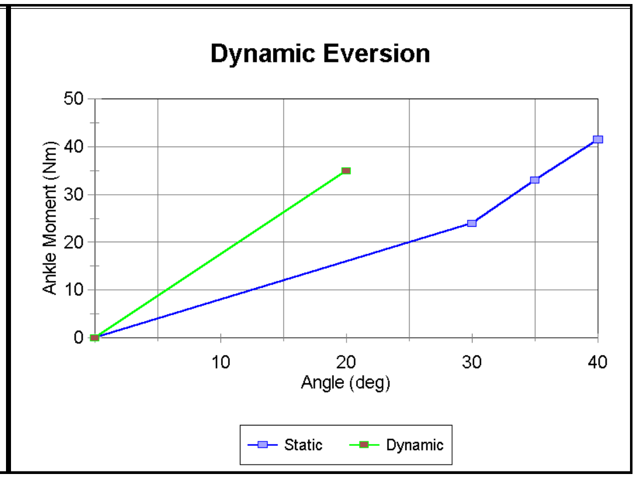


Figure 83. Moment vs angle response for dynamic eversion (and comparison with static).